Contents

Chapter 20

Waves in Cold Plasmas: Two-Fluid Formalism

Version 1120.2.K.pdf, 08 April 2011.
Please send comments, suggestions, and errata via email to kip@caltech.edu or on paper to Kip Thorne, 350-17 Caltech, Pasadena CA 91125

Box 20.1
Reader's Guide

- This chapter relies significantly on:
  - Chapter 19 on the particle kinetics of plasmas.
  - The basic concepts of fluid mechanics, Secs. 13.4 and 13.5.
  - Magnetosonic waves, Sec. 18.7.
  - The basic concepts of geometric optics, Secs. 7.2 and 7.3
- The remaining Chapters 21 and 22 of Part VI, Plasma Physics, rely heavily on this chapter.

20.1 Overview

The growth of plasma physics came about, historically, in the early 20th century, through studies of oscillations in electric discharges and the contemporaneous development of means to broadcast radio waves over great distances by reflecting them off the earth's ionosphere. It is therefore not surprising that most early plasma-physics research was devoted to describing the various modes of wave propagation. Even in the simplest, linear approximation for a plasma sufficiently cold that thermal effects are unimportant, we will see that the variety of possible modes is immense.

In the previous chapter, we introduced several length and time scales, e.g. the gyro (Larmor) radius, the Debye length, the plasma period, the gyro (cyclotron) period and the inverse collision frequency. To these we must now add the wavelength and period of the wave under study. The wave's characteristics are controlled by the relative sizes of these parameters; and in view of the large number of parameters, there is a bewildering number of possibilities. If we further recognize that plasmas are collisionless, so there is no guarantee that the particle distribution functions can be characterized by a single temperature, then the possibilities multiply.

Fortunately, the techniques needed to describe the propagation of linear wave perturbations in a particular equilibrium configuration of a plasma are straightforward and can be amply illustrated by studying a few simple cases. In this section, we shall follow this course by restricting our attention to one class of modes, those where we can either ignore completely the thermal motions of the ions and electrons that comprise the plasma (in other words treat these species as *cold*) or include them using just a velocity dispersion or temperature. We can then apply our knowledge of fluid dynamics by treating the ions and electrons separately as fluids, upon which act electromagnetic forces. This is called the *two-fluid formalism* for plasmas. In the next chapter, we shall show when and how waves are sensitive to the actual distribution of particle speeds by developing the more sophisticated *kinetic-theory formalism* and using it to study waves in *warm plasmas*.

We begin our two-fluid study of plasma waves in Sec. 20.2 by deriving a very general wave equation, which governs weak waves in a homogeneous plasma that may or may not have a magnetic field, and also governs electromagnetic waves in any other dielectric medium. That wave equation and the associated dispersion relation for the wave modes depend on a dielectric tensor, which must be derived from an examination of the motion of the electrons and protons (or other charge carriers) inside the wave.

In Sec. 20.4, we specialize to wave modes in a uniform, unmagnetized plasma. Using a two-fluid (electron-fluid and proton-fluid) description of the charge carriers' motions, we derive the dielectric tensor and thence the dispersion relation for the wave modes. The modes fall into two classes: (i) *Transverse or electromagnetic modes*. These are modified versions of electromagnetic waves in vacuum. As we shall see, they can propagate only at frequencies above the plasma frequency; at lower frequencies they become evanescent. (ii) *Longitudinal waves*, which come in two species: *Langmuir waves* and *ion acoustic waves*. Longitudinal waves are a melded combination of sound waves in a fluid and electrostatic plasma oscillations; their restoring force is a mixture of thermal pressure and electrostatic forces.

In Sec. 20.5, we explore how a uniform magnetic field changes the character of these waves. The $\mathbf{B}$ field makes the plasma anisotropic but axially symmetric. As a result, the dielectric tensor, dispersion relation, and wave modes have much in common with those in an anisotropic but axially symmetric dielectric crystal, which we studied in the context of nonlinear optics in Chap. 10. A plasma, however, has a much richer set of characteristic frequencies than does a crystal (electron plasma frequency, electron cyclotron frequency, ion cyclotron frequency, ...). As a result, even in the regime of weak linear waves and a cold plasma (no thermal pressure), the plasma has a far greater richness of modes than does a crystal.

In Sec. 20.5, we derive the general dispersion relation that encompasses all of these cold-magnetized-plasma modes, and explore the special cases of modes that propagate parallel to and perpendicular to the magnetic field. Then in Sec. 20.6 we examine a practical example: the propagation of radio waves in the Earth's ionosphere, where it is a good approximation to ignore the ion motion and work with a one-fluid (i.e. electron-fluid) theory. Having gained insight into simple cases (parallel modes, perpendicular modes, and one-fluid modes), we return in Sec. 20.7 to the full class of linear modes in a cold, magnetized, two-fluid plasma and briefly describe some tools by which one can make sense of them all.

Finally, in Sec. 20.8, we turn to the question of plasma stability. In Sec. 14.6 and Chap. 15, we saw that fluid flows that have sufficient shear are unstable; perturbations can feed off the relative kinetic energy of adjacent regions of the fluid, and use that energy to power an exponential growth. In plasmas, with their long mean free paths, there can similarly exist kinetic energies of relative, ordered, motion in velocity space; and perturbations, feeding off those energies, can grow exponentially. To study this in full requires the kinetic-theory description of a plasma, which we develop in Chap. 21; but in Sec. 20.8 we get insight into a prominent example of such a velocity-space instability by analyzing two cold plasma streams moving through each other. We illustrate the resulting *two-stream instability* by a short discussion of particle beams that are created in disturbances on the surface of the sun and propagate out through the solar wind.

20.2 Dielectric Tensor, Wave Equation, and General Dispersion Relation

We begin our study of waves in plasmas by deriving a very general wave equation which applies equally well to electromagnetic waves in unmagnetized plasmas, in magnetized plasmas, and in any other kind of dielectric medium such as an anisotropic crystal. This wave equation is the same one as we used in our study of nonlinear optics in Chap. 10 [Eqs. (10.42) and (10.43a)], and the derivation is essentially the same as that sketched in Ex. 10.7:

When a wave propagates through a plasma (or other dielectric), it entails a relative motion of electrons and protons (or other charge carriers). Assuming the wave has small enough amplitude to be linear, those charge motions can be embodied in an oscillating polarization (electric dipole moment per unit volume) $\mathbf{P}(\mathbf{x}, t)$, which is related to the plasma's (or dielectric's) varying charge density ρ_e and current density $\mathbf{j}$ in the usual way:

$$\boxed{\rho_e = -\boldsymbol{\nabla}\cdot\mathbf{P}\ , \quad \mathbf{j} = \frac{\partial \mathbf{P}}{\partial t}}\ . \tag{20.1}$$

(These relations enforce charge conservation, $\partial\rho_e/\partial t + \boldsymbol{\nabla}\cdot\mathbf{j} = 0$.) When these ρ_e and $\mathbf{j}$ are inserted into the standard Maxwell equations for $\mathbf{E}$ and $\mathbf{B}$, one obtains

$$\boxed{\boldsymbol{\nabla}\cdot\mathbf{E} = -\frac{\boldsymbol{\nabla}\cdot\mathbf{P}}{\epsilon_0}\ , \quad \boldsymbol{\nabla}\cdot\mathbf{B} = 0\ , \quad \boldsymbol{\nabla}\times\mathbf{E} = -\frac{\partial\mathbf{B}}{\partial t}\ , \quad \boldsymbol{\nabla}\times\mathbf{B} = \mu_0\frac{\partial\mathbf{P}}{\partial t} + \frac{1}{c^2}\frac{\partial\mathbf{E}}{\partial t}}\ . \tag{20.2}$$

If the plasma is endowed with a uniform magnetic field $\mathbf{B}_o$, that field can be left out of these

equations, as its divergence and curl are guaranteed to vanish. Thus, we can regard $\mathbf{E}$, $\mathbf{B}$ and $\mathbf{P}$ in these Maxwell equations as the perturbed quantities associated with the waves.

From a detailed analysis of the response of the charge carriers to the oscillating $\mathbf{E}$ and $\mathbf{B}$ fields, one can deduce a linear relationship between the waves' electric field $\mathbf{E}$ and the polarization $\mathbf{P}$,

$$\boxed{P_j = \epsilon_o \chi_{jk} E_k} \,. \tag{20.3}$$

Here ϵ_0 is the vacuum permittivity and χ_{jk} is a dimensionless, tensorial electric susceptibility [cf. Eq. (10.21)]. A different, but equivalent, viewpoint on the relationship between $\mathbf{P}$ and $\mathbf{E}$ can be deduced by taking the time derivative of Eq. (20.3), setting $\partial\mathbf{P}/\partial t = \mathbf{j}$, assuming a sinusoidal time variation $e^{-i\omega t}$ so $\partial\mathbf{E}/\partial t = -i\omega\mathbf{E}$, and then reinterpreting the result as Ohm's law with a tensorial electric conductivity $\kappa_{\mathrm{e}\,jk}$:

$$\boxed{j_j = \kappa_{\mathrm{e}\,jk} E_k \ , \quad \kappa_{\mathrm{e}\,jk} = -i\omega\epsilon_0\chi_{jk}} \,. \tag{20.4}$$

Evidently, for sinusoidal waves the electric susceptibility χ_{jk} and the electric conductivity $\kappa_{\mathrm{e}\,jk}$ embody the same information about the wave-particle interactions.

That information is also embodied in a third object: the dimensionless dielectric tensor ϵ_{jk}, which relates the electric displacement $\mathbf{D}$ to the electric field $\mathbf{E}$:

$$\boxed{D_j \equiv \epsilon_0 E_j + P_j = \epsilon_0 \epsilon_{jk} E_k \ , \quad \epsilon_{jk} = \delta_{jk} + \chi_{jk} = \delta_{jk} + \frac{i}{\epsilon_0\omega}\kappa_{\mathrm{e}\,jk}} \,. \tag{20.5}$$

In the next section we shall derive the value of the dielectric tensor ϵ_{jk} for waves in an unmagnetized plasma, and in Sec. 20.4 we shall derive it for a magnetized plasma.

Using the definition $\mathbf{D} = \epsilon_0\mathbf{E} + \mathbf{P}$, we can eliminate $\mathbf{P}$ from equations (20.2), thereby obtaining the familiar form of Maxwell's equations for dielectric media with no non-polarization-based charges or currents:

$$\boldsymbol{\nabla}\cdot\mathbf{D} = 0 \ , \quad \boldsymbol{\nabla}\cdot\mathbf{B} = 0 \ , \quad \boldsymbol{\nabla}\times\mathbf{E} = -\frac{\partial\mathbf{B}}{\partial t} \ , \quad \boldsymbol{\nabla}\times\mathbf{B} = \mu_0\frac{\partial\mathbf{D}}{\partial t} \ . \tag{20.6}$$

By taking the curl of the third of these equations and combining with the fourth and with $D_j = \epsilon_0\epsilon_{jk}E_k$, we obtain the wave equation that governs the perturbations:

$$\nabla^2\mathbf{E} - \boldsymbol{\nabla}(\boldsymbol{\nabla}\cdot\mathbf{E}) - \boldsymbol{\epsilon}\cdot\frac{1}{c^2}\frac{\partial^2\mathbf{E}}{\partial t^2} = 0 \ , \tag{20.7}$$

where $\boldsymbol{\epsilon}$ is our index-free notation for ϵ_{jk}. Specializing to a plane-wave mode with wave vector $\mathbf{k}$ and angular frequency ω, so $\mathbf{E} \propto e^{i\mathbf{k}\mathbf{x}}e^{-i\omega t}$, we convert this wave equation into a homogeneous algebraic equation for the Cartesian components of the electric vector E_j (cf. Box 12.2):

$$\boxed{L_{ij}E_j = 0} \,, \tag{20.8}$$

where

$$\boxed{L_{ij} = k_i k_j - k^2\delta_{ij} + \frac{\omega^2}{c^2}\epsilon_{ij}} \,. \tag{20.9}$$

The algebratized wave equation (20.8) can have a solution only if the determinant of the three-dimensional matrix L_{ij} vanishes:

$$\boxed{\det||L_{ij}|| \equiv \det\left|\left|k_i k_j - k^2\delta_{ij} + \frac{\omega^2}{c^2}\epsilon_{ij}\right|\right|}. \tag{20.10}$$

This is a polynomial equation for the angular frequency as a function of the wave vector (with ω and $\mathbf{k}$ appearing not only explicitly in L_{ij} but also implicitly in the functional form of ϵ_{jk}). Each solution, $\omega(\mathbf{k})$, of this equation is the dispersion relation for a particular wave mode. We therefore can regard Eq. (20.10) as the general dispersion relation for plasma waves—and for linear electromagnetic waves in any other kind of dielectric medium.

To obtain an explicit form of the dispersion relation (20.10), we must give a prescription for calculating the dielectric tensor ϵ_{ij}, or equivalently [cf. Eq. (20.5)] the conductivity tensor $\kappa_{\mathrm{e}\,ij}$ or the susceptibility tensor χ_{ij}. The simplest prescription involves treating the electrons and ions as independent fluids; so we shall digress, briefly, from our discussion of waves, to present the two-fluid formalism for plasmas:

20.3 Two-Fluid Formalism

A plasma necessarily contains rapidly moving electrons and ions, and their individual responses to an applied electromagnetic field depend on their velocities. In the simplest model of these responses, we average over all the particles in a species (electrons or protons in this case) and treat them collectively as a fluid. Now, the fact that all the electrons are treated as one fluid does not mean that they have to collide with one another. In fact, as we have already emphasized in Chap. 19, electron-electron collisions are usually quite rare and we can usually ignore them. Nevertheless, we can still define a mean fluid velocity for both the electrons and the protons by averaging over their total velocity distribution functions just as we would for a gas:

$$\boxed{\mathbf{u}_s = \langle \mathbf{v} \rangle_s \; ; \quad s = p, e}, \tag{20.11}$$

where the subscripts p and e refer to protons and electrons. Similarly, for each fluid we define a pressure tensor using the fluid's dispersion of particle velocities:

$$\boxed{\mathbf{P}_s = n_s m_s \langle (\mathbf{v} - \mathbf{u}_s) \otimes (\mathbf{v} - \mathbf{u}_s) \rangle} \tag{20.12}$$

[cf. Eqs. (19.42) and (19.43)].

The density n_s and mean velocity $\mathbf{u}_s$ of each species s must satisfy the equation of continuity (particle conservation)

$$\boxed{\frac{\partial n_s}{\partial t} + \boldsymbol{\nabla} \cdot (n_s \mathbf{u}_s) = 0}. \tag{20.13a}$$

They must also satisfy an equation of motion: the law of momentum conservation, i.e., the Euler equation with the Lorentz force added to the right side

$$\boxed{n_s m_s \left(\frac{\partial \mathbf{u}_s}{\partial t} + (\mathbf{u}_s \cdot \nabla)\mathbf{u}_s \right) = -\boldsymbol{\nabla} \cdot \mathbf{P}_s + n_s q_s (\mathbf{E} + \mathbf{u}_s \times \mathbf{B})}. \tag{20.13b}$$

Here we have neglected the tiny influence of collisions between the two species. In these equations and below, $q_s = \pm e$ is the particles' charge (positive for protons and negative for electrons). Note that, as collisions are ineffectual, we cannot assume that the pressure tensor is isotropic.

Although the continuity and momentum-conservation equations (20.13) for each species (electron or proton) is formally decoupled from the equations for the other species, there is actually a strong physical coupling induced by the electromagnetic field: The two species jointly produce $\mathbf{E}$ and $\mathbf{B}$ through their joint charge density and current density

$$\boxed{\rho_e = \sum_s q_s n_s \ , \quad \mathbf{j} = \sum_s q_s n_s \mathbf{u}_s} \ , \tag{20.14}$$

and those $\mathbf{E}$ and $\mathbf{B}$ strongly influence the electron and proton fluids' dynamics via their equations of motion (20.13b).

****

EXERCISES

Exercise 20.1 *Problem: Fluid Drifts in a Time-Independent, Magnetized Plasma*
Consider a hydrogen plasma described by the two-fluid formalism. Suppose that Coulomb collisions have had time to isotropize the electrons and protons and to equalize their temperatures so that their partial pressures $P_e = n_e k_B T$ and $P_p = n_p k_B T$ are isotropic and equal. An electric field $\mathbf{E}$ created by external charges is applied.

(a) Using the law of force balance for fluid s, show that its drift velocity perpendicular to the magnetic field is

$$v_{s\perp} = \frac{\mathbf{E}\times\mathbf{B}}{B^2} - \frac{\boldsymbol{\nabla} P_s \times \mathbf{B}}{q_s n_s B^2} - \frac{m_s}{q_s B^2}[(\mathbf{v}_s\cdot\boldsymbol{\nabla})\mathbf{v}_s]_\perp \times \mathbf{B} \ . \tag{20.15}$$

The first term is the $\mathbf{E}\times\mathbf{B}$ drift discussed in Sec. 19.7.1.

(b) The second term, called the "diamagnetic drift", is different for the electrons and the protons. Show that this drift produces a current density perpendicular to $\mathbf{B}$ given by

$$\mathbf{j}_\perp = -\frac{(\boldsymbol{\nabla} P)\times\mathbf{B}}{B^2} \ , \tag{20.16}$$

where P is the total pressure.

(c) The third term in Eq. (20.15) can be called the "drift-induced drift". Show that, if the electrons are nearly locked to the ion motion, then the associated current density is well approximated by

$$\mathbf{j}_\perp = -\frac{\rho}{B^2}[(\mathbf{v}\cdot\boldsymbol{\nabla})\mathbf{v}]\times\mathbf{B} \ , \tag{20.17}$$

where ρ is the mass density and $\mathbf{v}$ is the average fluid speed.

The transverse current densities (20.16) and (20.17) can also be derived by crossing $\mathbf{B}$ into the MHD equation of force balance (18.11) for a time-independent, magnetized plasma.

****

20.4 Wave Modes in an Unmagnetized Plasma

We now specialize to waves in a homogeneous, unmagnetized electron-proton plasma.

Consider, first, an unperturbed plasma in the absence of a wave, and work in a frame in which the proton fluid velocity $\mathbf{u}_p$ vanishes. By assumption, the equilibrium is spatially uniform. If there were an electric field, then charges would quickly flow to neutralize it; so there can be no electric field, and hence (since $\boldsymbol{\nabla}\cdot\mathbf{E} = \rho_e/\epsilon_0$) no net charge density. Therefore, the electron density must equal the proton density. Furthermore, there can be no net current as this would lead to a magnetic field; so since the proton current $e\,n_p\mathbf{u}_p$ vanishes, the electron current $= -e\,n_e\mathbf{u}_e$ must also vanish, whence the electron fluid velocity $\mathbf{u}_e$ must vanish in our chosen frame. In summary: *in an equilibrium homogeneous, unmagnetized plasma,* $\mathbf{u}_e$*,* $\mathbf{u}_p$*,* $\mathbf{E}$ *and* $\mathbf{B}$ *all vanish.*

Now apply an electromagnetic perturbation. This will induce a small, oscillating fluid velocity $\mathbf{u}_s$ in both the proton and electron fluids. It should not worry us that the fluid velocity is small compared with the random speeds of the constituent particles; the same is true in any subsonic gas dynamical flow, but the fluid description remains good there and so also here.

20.4.1 Dielectric Tensor and Dispersion Relation for a Cold, Unmagnetized Plasma

Continuing to keep the plasma unmagnetized, let us further simplify matters (temporarily) by restricting ourselves to a cold plasma, so the tensorial pressures vanish, $\mathbf{P}_s = 0$. As we are only interested in linear wave modes, we rewrite the two-fluid equations (20.13) just retaining terms that are first order in perturbed quantities, i.e. dropping the $(\mathbf{u}_s\cdot\boldsymbol{\nabla})\mathbf{u}_s$ and $\mathbf{u}_s\times\mathbf{B}$ terms. Then, focusing on a plane-wave mode, $\propto \exp[i(\mathbf{k}\cdot\mathbf{x}-\omega t)]$, we bring the equation of motion (20.13b) into the form

$$\boxed{-i\omega n_s m_s \mathbf{u}_s = q_s n_s \mathbf{E}} \tag{20.18}$$

for each species, $s = p, e$. From this, we can immediately deduce the linearized current density

$$\mathbf{j} = \sum_s n_s q_s \mathbf{u}_s = \sum_s \frac{i n_s q_s^2}{m_s\omega}\mathbf{E}\ , \tag{20.19}$$

from which we infer that the conductivity tensor $\boldsymbol{\kappa}_{\rm e}$ has Cartesian components

$$\kappa_{{\rm e}\,ij} = \sum_s \frac{i n_s q_s^2}{m_s\omega}\delta_{ij}\ , \tag{20.20}$$

where δ_{ij} is the Kronecker delta. Note that the conductivity is purely imaginary, which means that the current oscillates out of phase with the applied electric field, which in turn implies that there is no time-averaged ohmic energy dissipation, $\langle\mathbf{j}\cdot\mathbf{E}\rangle = 0$. Inserting the conductivity tensor (20.20) into the general equation (20.5) for the dielectric tensor, we obtain

$$\epsilon_{ij} = \delta_{ij} + \frac{i}{\epsilon_0\omega}\kappa_{{\rm e}\,ij} = \left(1 - \frac{\omega_p^2}{\omega^2}\right)\delta_{ij}\ . \tag{20.21}$$

Here and throughout this chapter, the plasma frequency ω_p is very slightly different from that used in Chap. 19: it includes a tiny (1/1836) correction due to the motion of the protons, which we neglected in our analysis of plasma oscillations in Sec. 19.3.3:

$$\boxed{\omega_p^2 = \sum_s \frac{n_s q_s^2}{m_s \epsilon_0} = \frac{n e^2}{m_e \epsilon_0}\left(1 + \frac{m_e}{m_p}\right)}. \tag{20.22}$$

Note that because there is no physical source of a preferred direction in the plasma, the dielectric tensor (20.21) is isotropic.

Now, without loss of generality, let the waves propagate in the z direction, so $\mathbf{k} = k\mathbf{e}_z$. Then the algebratized wave operator (20.9), with $\boldsymbol{\epsilon}$ given by (20.21), takes the following form:

$$\boxed{L_{ij} = \frac{\omega^2}{c^2}\begin{pmatrix} 1 - \frac{c^2k^2}{\omega^2} - \frac{\omega_p^2}{\omega^2} & 0 & 0 \\ 0 & 1 - \frac{c^2k^2}{\omega^2} - \frac{\omega_p^2}{\omega^2} & 0 \\ 0 & 0 & 1 - \frac{\omega_p^2}{\omega^2} \end{pmatrix}}. \tag{20.23}$$

The corresponding dispersion relation $\det||L_{jk}|| = 0$ becomes

$$\left(1 - \frac{c^2k^2}{\omega^2} - \frac{\omega_p^2}{\omega^2}\right)^2 \left(1 - \frac{\omega_p^2}{\omega^2}\right) = 0\,. \tag{20.24}$$

This is a polynomial equation of order 6 for ω as a function of k, so formally there are six solutions corresponding to three pairs of modes propagating in opposite directions.

Two of the pairs of modes are degenerate with frequency

$$\boxed{\omega = \sqrt{\omega_p^2 + c^2k^2}\,.}. \tag{20.25}$$

We shall study them in the next subsection. The remaining pair of modes exist at a single frequency,

$$\boxed{\omega = \omega_p} \tag{20.26}$$

These must be the electrostatic plasma oscillations that we studied in Sec. 19.3.3 (though now with an arbitrary wave number k, while in Sec. 19.3.3 the wave number was assumed zero.) In Sec. 20.4.3 we shall show that this is so and shall explore how these plasma oscillations get modified by finite-temperature effects.

20.4.2 Electromagnetic Plasma Waves

To learn the physical nature of the modes with dispersion relation $\omega = \sqrt{\omega_p^2 + c^2k^2}$ [Eq. (20.25)], we must examine the details of their electric-field oscillations, magnetic-field oscillations, and electron and proton motions. A key to this is the algebratized wave equation $L_{ij}E_j = 0$, with L_{ij} specialized to the dispersion relation (20.25): $||L_{ij}|| = \mathrm{diag}[0, 0, (\omega^2 - \omega_p^2)/c^2]$. In this case, the general solution to $L_{ij}E_j = 0$ is an electric field that lies in the x–y plane

(transverse plane), i.e. that is orthogonal to the waves' propagation vector $\mathbf{k} = k\mathbf{e}_z$. The third of the Maxwell equations (20.2) implies that the magnetic field is

$$\mathbf{B} = (\mathbf{k}/\omega) \times \mathbf{E} \,, \tag{20.27}$$

which also lies in the transverse plane and is orthogonal to $\mathbf{E}$. Evidently, these modes are close analogs of electromagnetic waves in vacuum; correspondingly, they are known as the plasma's *electromagnetic modes*. The electron and proton motions in these modes, as given by Eq. (20.18), are oscillatory displacements in the direction of $\mathbf{E}$ but out of phase with $\mathbf{E}$. The amplitudes of the fluid motions vary as $1/\omega$; as ω decreases, the fluid amplitudes grow.

The dispersion relation for these modes, Eq. (20.25), implies that they can only propagate (i.e. have real angular frequency when the wave vector is real) if ω exceeds the plasma frequency. As ω is decreased toward ω_p, k approaches zero, so these modes become electrostatic plasma oscillations with arbitrarily long wavelength orthogonal to the oscillation direction, i.e., they become a spatially homogeneous variant of the plasma oscillations studied in Sec. 19.3.3. At $\omega < \omega_p$ these modes become evanescent.

In their regime of propagation, $\omega > \omega_p$, these cold-plasma electromagnetic waves have a phase velocity given by

$$\mathbf{V}_{\rm ph} = \frac{\omega}{k}\hat{\mathbf{k}} = c\left(1 - \frac{\omega_p^2}{\omega^2}\right)^{-1/2} \hat{\mathbf{k}} \,, \tag{20.28}$$

where $\hat{\mathbf{k}} \equiv \mathbf{k}/k$ is a unit vector in the propagation direction. Although this phase velocity exceeds the speed of light, causality is not violated because information (and energy) propagate at the group velocity, not the phase velocity. The group velocity is readily shown to be

$$\mathbf{V}_g = \nabla_{\mathbf{k}}\,\omega = \frac{c^2\mathbf{k}}{\omega} = c\left(1 - \frac{\omega_p^2}{\omega^2}\right)^{1/2} \hat{\mathbf{k}} \,, \tag{20.29}$$

which is less than c.

These cold-plasma electromagnetic modes transport energy and momentum just like wave modes in a fluid. There are three contributions to the waves' mean (time-averaged) energy density: the electric, the magnetic and the kinetic energy densities. (If we had retained the pressure, then there would have been an additional contribution from the internal energy.) In order to compute these mean energy densities, we must form the time average of products of physical quantities. Now, we have used the complex representation to denote each of our oscillating quantities (e.g. E_x), so we must be careful to remember that $A = ae^{i(\mathbf{k}\cdot\mathbf{x}-\omega t)}$ is an abbreviation for the real part of this quantity—which is the physical A. It is easy to show that the time-averaged value of the physical A times the physical B (which we shall denote by $\langle AB\rangle$) is given in terms of their complex amplitudes by

$$\langle AB\rangle = \frac{AB^* + A^*B}{4} \,. \tag{20.30}$$

Using Eqs. (20.27) and (20.28), we can write the magnetic energy density in the form $\langle B^2\rangle/2\mu_0 = (1-\omega_p^2/\omega^2)\epsilon_0\langle E^2\rangle/2$. Using Eq. (20.19), the electron kinetic energy is $n_e m_e\langle u_e^2\rangle/2 =$

$(\omega_{pe}^2/\omega^2)\epsilon_0\langle E^2\rangle/2$ and likewise for the proton kinetic energy. Summing these contributions and using Eq. (20.30), we obtain

$$\begin{aligned} U &= \frac{\epsilon_0 E E^*}{4} + \frac{B B^*}{4\mu_0} + \sum_s \frac{n_s m_s u_s u_s^*}{4} \\ &= \frac{\epsilon_0 E E^*}{2} \ . \end{aligned} \tag{20.31}$$

The mean energy flux in the wave is carried (to quadratic order) by the electromagnetic field and is given by the Poynting flux. (The kinetic-energy flux vanishes to this order.) A straightforward calculation gives

$$\begin{aligned} \mathbf{F}_{\rm EM} &= \langle \mathbf{E}\times\mathbf{B}\rangle = \frac{\mathbf{E}\times\mathbf{B}^* + \mathbf{E}^*\times\mathbf{B}}{4} = \frac{E E^* \mathbf{k}}{2\mu_0\omega} \\ &= U V_g \ , \end{aligned} \tag{20.32}$$

where we have used $\mu_0 = c^{-2}\epsilon_0^{-1}$. We therefore find that the energy flux is the product of the energy density and the group velocity, as is true quite generally; cf. Sec. 6.3. (If it were not true, then a localized wave packet, which propagates at the group velocity, would move along a different trajectory from its energy, and we would wind up with energy in regions with vanishing amplitude!)

20.4.3 Langmuir Waves and Ion Acoustic Waves in Warm Plasmas

For our case of a cold, unmagnetized plasma, the third pair of modes embodied in the dispersion relation (20.24) only exists at a single frequency, the plasma frequency $\omega = \omega_p$. These modes' wave equation $L_{ij}E_j = 0$ with $||L_{ij}|| = \mathrm{diag}(-k^2, -k^2, 0)$ [Eq. (20.23) with $\omega^2 = \omega_p^2$] implies that $\mathbf{E}$ points in the z-direction, i.e., along $\mathbf{k}$, i.e. in the *longitudinal direction.* The Maxwell equations then imply $\mathbf{B} = 0$, and the equation of motion (20.18) implies that the fluid displacements are in the direction of $\mathbf{E}$ — the longitudinal direction. Clearly, these modes, like electromagnetic modes in the limit $k = 0$ and $\omega = \omega_p$, are electrostatic plasma oscillations. However, in this case, where the spatial variations of $\mathbf{E}$ and $\mathbf{u}_s$ are along the direction of oscillation instead of perpendicular, k is not constrained to vanish; rather, all wave numbers are allowed. This means that the plasma can undergo plane-parallel oscillations at $\omega = \omega_p$ with displacements in some Cartesian z-direction, and any arbitrary z-dependent amplitude that one might wish. But these oscillations cannot transport energy; because ω is independent of $\mathbf{k}$, their group velocity $\mathbf{V}_g = \nabla_{\mathbf{k}}\,\omega$ vanishes.

So far, we have confined ourselves to wave modes in cold plasmas and have ignored thermal motions of the particles. When thermal motions are turned on, the resulting thermal pressure gradients convert longitudinal plasma oscillations, at finite wave number k, into propagating, energy-transporting, longitudinal modes called *Langmuir waves.* As we have already intimated, because the plasma is collisionless, to understand the thermal effects fully we must turn to kinetic theory (Chap. 21). However, within the present chapter's two-fluid formalism, we can deduce the leading order effects of finite temperature with the guidance of physical arguments.

In our physical arguments, we shall assume that the electrons are thermalized with each other at a temperature T_e, the protons are thermalized at temperature T_p, and T_e and T_p may differ (because the timescale for electrons and protons to exchange energy is so much longer than the timescales for electrons to exchange energy among themselves and for protons to exchange energy among themselves; see Sec. 19.4.3.

Physically, the key to the Langumir waves' propagation is the warm electrons' thermal pressure. (The proton pressure is unimportant because the protons oscillate electrostatically with an amplitude that is tiny compared to the electrons; nevertheless, as we shall see below, the proton pressure is important in other ways.)

Now, in an adiabatic sound wave *in a fluid* (where the particle mean free paths are small compared to the wavelength), we relate the pressure perturbation to the density perturbation by assuming that the entropy is held constant. In other words, we write $\boldsymbol{\nabla} P = C^2 m \boldsymbol{\nabla} n$, where $C = (\gamma P/nm)^{1/2}$ is the adiabatic sound speed (not to be confused with the speed of light c), n is the particle density, m is the particle mass, and γ is the specific heat ratio, which is 5/3 for a monatomic gas.

However, the electron gas *in the plasma we are considering* is collisionless on the short timescale of a perturbation period, and we are only interested in the tensorial pressure gradient parallel to $\mathbf{k}$ (which we take to point in the z direction), $\delta P_{e\,zz,z}$. We can therefore ignore all electron motion perpendicular to the wave vector as this is not coupled to the parallel motion. The electron motion is then effectively one dimensional as there is only one (translational) degree of freedom. The relevant specific heat at constant volume is therefore just $k_B/2$ per electron, while that at constant pressure is $3k_B/2$, giving $\gamma = 3$.[1] The effective sound speed for the electron gas is then $C = (3k_B T_e/m_e)^{1/2}$, and correspondingly the perturbations of longitudinal electron pressure and electron density are related by

$$\frac{\delta P_{e\,zz}}{m_e \delta n_e} = C^2 = \frac{3k_B T_e}{m_e} \ . \tag{20.33a}$$

This is one of the equations governing Langmuir waves. The others are the linearized equation of continuity (20.13a), which relates the electrons' density perturbation to the longitudinal component of their fluid velocity perturbation

$$\delta n_e = n_e \frac{k}{\omega} u_{e\,z} \ , \tag{20.33b}$$

the linearized equation of motion (20.13b), which relates $u_{e\,z}$ and $\delta P_{e\,zz}$ to the longitudinal component of the oscillating electric field

$$-i\omega n_e m_e u_{e\,z} = ik\delta P_{e\,zz} - n_e e E_z \ , \tag{20.33c}$$

and the linearized form of Poisson's equation $\boldsymbol{\nabla} \cdot \mathbf{E} = \rho_e/\epsilon_0$, which relates E_z to δn_e

$$ikE_z = -\frac{\delta n_e e}{\epsilon_0} \ . \tag{20.33d}$$

[1] We derived this longitudinal adiabatic index $\gamma = 3$ by a different method in Ex. 19.11e [Eq. (19.45)] in the context of a plasma with a magnetic field along the longitudinal, z direction; it is valid also in our unmagnetized case because the magnetic field has no influence on longitudinal electron motions.

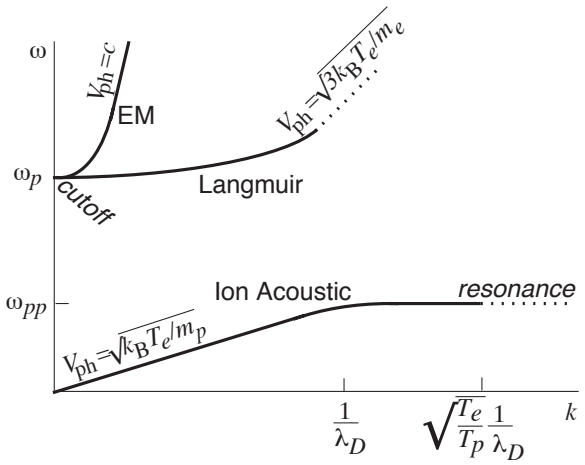

Fig. 20.1: Dispersion relations for electromagnetic waves, Langmuir waves, and ion-acoustic waves in an unmagnetized plasma, whose electrons are thermalized with each other at temperature T_e, and protons are thermalized at a temperature T_p that might not be equal to T_e. In the dotted regions the waves are strongly damped, according to kinetic-theory analyses in Chap. 21.

Equations (20.33) are four equations for three ratios of the perturbed quantities. By combining these equations, we obtain a condition that must be satisfied in order for them to have a solution:

$$\boxed{\omega^2 = \omega_{pe}^2 + \frac{3k_BT_e}{m_e}k^2 = \omega_{pe}^2(1+3k^2\lambda_D^2)}\ ; \tag{20.34}$$

here $\lambda_D = \sqrt{\epsilon_0 k_B T_e/n_e e^2}$ is the Debye length [Eq. (19.10)]. Equation (20.34) is the *Bohm-Gross* dispersion relation for Langmuir waves.

From this dispersion relation we deduce the phase speed of a Langmuir wave:

$$V_{\rm ph} = \frac{\omega}{k} = \left(\frac{k_BT_e}{m_e}\right)^{1/2}\left(3+\frac{1}{k^2\lambda_D^2}\right)^{1/2}\ . \tag{20.35}$$

Evidently, when the reduced wavelength $\lambda/2\pi = 1/k$ is less than or of order the Debye length ($k\lambda_D \gtrsim 1$), the phase speed becomes comparable with the electron thermal speed. It is then possible for individual electrons to transfer energy between adjacent compressions and rarefactions in the wave. As we shall see in the next chapter, when we recover Eq. (20.34) from a kinetic treatment, the resulting energy transfers damp the wave. Therefore, the Bohm-Gross dispersion relation is only valid for reduced wavelengths much longer than the Debye length, i.e. $k\lambda_D \ll 1$; cf. Fig. 20.1.

In our analysis of Langmuir waves, we have ignored the proton motion. This is justified as long as the proton thermal speeds are small compared to the electron thermal speeds, i.e. $T_p \ll m_pT_e/m_e$, which will almost always be the case. Proton motion is, however, not ignorable in a second type of plasma wave that owes its existence to finite temperature: *ion acoustic waves*. These are waves that propagate with frequencies far below the electron plasma frequency—frequencies so low that the electrons remain locked electrostatically to

the protons, keeping the plasma charge neutral and preventing electromagnetic fields from participating in the oscillations. As for Langmuir waves, we can derive the ion-acoustic dispersion relation using fluid theory combined with physical arguments:

In the next chapter, using kinetic theory we shall see that ion acoustic waves can propagate only when the proton temperature is very small compared with the electron temperature, $T_p \ll T_e$; otherwise they are damped. (Such a temperature disparity is produced, e.g., when a plasma passes through a shock wave, and it can be maintained for a long time because Coulomb collisions are so ineffective at restoring $T_p \sim T_e$; cf. Sec. 19.4.3.) Because $T_p \ll T_e$, the proton pressure can be ignored and the waves' restoring force is provided by electron pressure. Now, in an ion acoustic wave, by contrast with a Langmuir wave, the individual thermal electrons can travel over many wavelengths during a single wave period, so the electrons remain isothermal as their mean motion oscillates in lock-step with the protons' mean motion. Correspondingly, the electrons' effective (one-dimensional) specific heat ratio is $\gamma_{\rm eff} = 1$.

Although the electrons provide the ion-acoustic waves' restoring force, the inertia of the electrostatically-locked electrons and protons is almost entirely that of the heavy protons. Correspondingly, the waves' phase velocity is

$$\mathbf{V}_{ia} = \left(\frac{\gamma_{\rm eff} P_e}{n_p m_p}\right)^{1/2} \hat{k} = \left(\frac{k_B T_e}{m_p}\right)^{1/2} \hat{k} \ , \tag{20.36}$$

(cf. Ex. 20.4) and the dispersion relation is $\omega = V_{\rm ph} k = (k_B T_e/m_p)^{1/2} k$.

From this phase velocity and our physical description of these ion-acoustic waves, it should be evident that they are the magnetosonic waves of MHD theory (Sec. 18.7.2), in the limit that the plasma's magnetic field is turned off.

In Ex. 20.4, we show that the character of these waves gets modified when their wavelength becomes of order the Debye length, i.e. when $k\lambda_D \sim 1$. The dispersion relation then gets modified to

$$\boxed{\omega = \left(\frac{k_B T_e/m_p}{1+\lambda_D^2 k^2}\right)^{1/2} k} \ , \tag{20.37}$$

which means that for $k\lambda_D \gg 1$, the waves' frequency approaches the *proton plasma frequency* $\omega_{pp} \equiv \sqrt{ne^2/\epsilon_0 m_p} \simeq \sqrt{m_e/m_p}\omega_p$. A kinetic-theory treatment reveals that these waves are strong damped when $k\lambda_D \gtrsim \sqrt{T_e/T_p}$. These features of the ion-acoustic dispersion relation are shown in Fig. 20.1.

20.4.4 Cutoffs and Resonances

Electromagnetic waves, Langmuir waves and ion-acoustic waves in an unmagnetized plasma provide examples of *cutoffs* and *resonances*.

A *cutoff* is a frequency at which a wave mode ceases to propagate, because its wave number k there becomes zero. Langmuir and electromagnetic waves at $\omega \to \omega_p$ are examples; see their dispersion relations plotted in Fig. 20.1. Consider, for concreteness, a monochromatic radio-frequency electromagnetic wave propagating upward into the earth's ionosphere

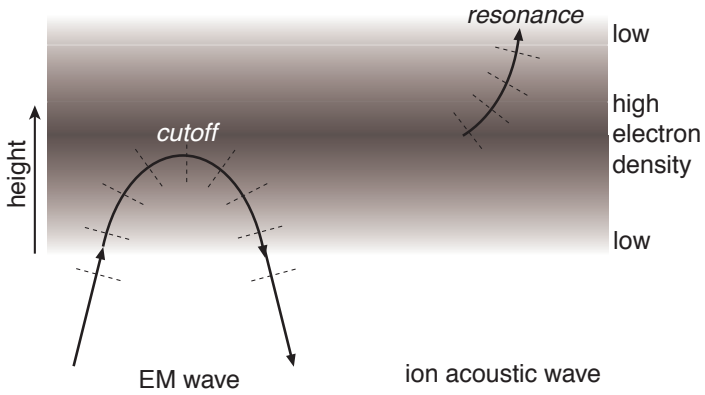

Fig. 20.2: Cutoff and resonance illustrated by wave propagation in the Earth's ionosphere. The thick, arrowed curves are rays and the thin, dashed curves are phase fronts. The electron density is proportional to the darkness of the shading.

at some nonzero angle to the vertical (left side of Fig. 20.2), and neglect the effects of the earth's magnetic field. As the wave moves deeper (higher) into the ionosphere, it encounters a rising electron density n and correspondingly a rising plasma frequency ω_p. The wave's wavelength will typically be small compared to the inhomogeneity scale for ω_p, so the wave propagation can be analyzed using geometric optics (Sec. 7.3). Across a phase front, that portion which is higher in the ionosphere will have a smaller k and thus a larger wavelength and phase speed, and thus a greater distance between phase fronts (dashed lines). Therefore, the rays, which are orthogonal to the phase fronts, will bend away from the vertical (left side of Fig. 20.2); i.e., the wave will be reflected away from the cutoff at which $\omega_p \to \omega$ and $k \to 0$. Clearly, this behavior is quite general. *Wave modes are generally reflected from regions in which slowly changing plasma conditions give rise to cutoffs.*

A *resonance* is a frequency at which a wave mode ceases to propagate because its wave number k there becomes infinite, i.e. its wavelength goes to zero. Ion-acoustic waves provide an example; see their dispersion relation in Fig. 20.1. Consider, for concreteness, an ion-acoustic wave deep within the ionosphere, where ω_{pp} is larger than the wave's frequency ω (right side of Fig. 20.2). As the wave propagates toward the upper edge of the ionosphere, at some nonzero angle to the vertical, the portion of a phase front that is higher sees a smaller electron density and thus a smaller ω_{pp}, and thence has a larger k and shorter wavelength, and thus a shorter distance between phase fronts (dashed lines). This causes the rays to bend toward the vertical (right side of Fig. 20.2). The wave is "attracted" into the region of the resonance, $\omega \to \omega_{pp}$, $k \to \infty$, where it gets "Landau damped" (Chap. 21) and dies. This behavior is quite general. *Wave modes are generally attracted toward regions in which slowly changing plasma conditions give rise to resonances, and upon reaching a resonance, they die.*

We shall study wave propagation in the ionosphere in greater detail in Sec. 20.6 below.

****

EXERCISES

Exercise 20.2 *Derivation: Time-average Formula*
Verify Eq. (20.30).

Exercise 20.3 *Example: Collisional Damping in an Electromagnetic Wave Mode*
Consider a transverse electromagnetic wave mode propagating in an unmagnetized, partially ionized gas in which the electron-neutral collision frequency is ν_e. Include the effects of collisions in the electron equation of motion, Eq. (20.18), by introducing a term $-n_e m_e \nu_e \mathbf{u}_e$ on the right hand side. Ignore ion motion and electron-ion and electron-electron collisions.

Derive the dispersion relation when $\omega \gg \nu_e$ and show by explicit calculation that the rate of loss of energy per unit volume ($-\boldsymbol{\nabla} \cdot \mathbf{F}_{\rm EM}$, where $\mathbf{F}_{\rm EM}$ is the Poynting flux) is balanced by the Ohmic heating of the plasma. (Hint: It may be easiest to regard ω as real and $\mathbf{k}$ as complex.)

Exercise 20.4 *Derivation: Ion Acoustic Waves*
Ion acoustic waves can propagate in an unmagnetized plasma when the electron temperature T_e greatly exceeds the ion temperature T_p. In this limit, the electron density n_e can be approximated by $n_e = n_0 \exp(e\Phi/k_B T_e)$, where n_0 is the mean electron density and Φ is the electrostatic potential.

(a) Show that for ion-acoustic waves that propagate in the z direction, the nonlinear equations of continuity and motion for the ion (proton) fluid and Poisson's equation for the potential take the form

$$\begin{aligned} \frac{\partial n}{\partial t} + \frac{\partial (nu)}{\partial z} &= 0 \ , \\ \frac{\partial u}{\partial t} + u\frac{\partial u}{\partial z} &= -\frac{e}{m_p}\frac{\partial \Phi}{\partial z} \ , \\ \frac{\partial^2 \Phi}{\partial z^2} &= -\frac{e}{\epsilon_0}(n - n_0 e^{e\Phi/k_B T_e}) \ . \end{aligned} \tag{20.38}$$

Here n is the proton density and u is the proton fluid velocity (which points in the z direction).

(b) Linearize these equations and show that the dispersion relation for small-amplitude ion acoustic modes is

$$\omega = \omega_{pp}\left(1 + \frac{1}{\lambda_D^2 k^2}\right)^{-1/2} = \left(\frac{k_B T_e/m_p}{1 + \lambda_D^2 k^2}\right)^{1/2} k \ , \tag{20.39}$$

where λ_D is the Debye length. Verify that in the long-wavelength limit, this agrees with Eq. (20.36).

Exercise 20.5 *Challenge: Ion Acoustic Solitons*
In this exercise we shall explore nonlinear effects in ion acoustic waves (Ex. 20.4), and shall show that they give rise to solitons that obey the same Korteweg-de Vries equation as governs solitonic water waves (Sec. 16.3).

(a) Introduce a bookkeeping expansion parameter ε whose numerical value is unity,[2] and expand the ion density, ion velocity and potential in the form

$$\begin{aligned} n &= n_0(1 + \varepsilon n_1 + \varepsilon^2 n_2 + \dots) \ , \\ u &= (k_B T_e/m_p)^{1/2}(\varepsilon u_1 + \varepsilon^2 u_2 + \dots) \ , \\ \Phi &= (k_B T_e/e)(\varepsilon \Phi_1 + \varepsilon^2 \Phi_2 + \dots) \ . \end{aligned} \tag{20.40}$$

Here n_1, u_1, Φ_1 are small compared to unity, and the factors of ε tell us that, as the wave amplitude is decreased, these quantities scale proportionally to each other, while n_2, u_2, and Φ_2 scale proportionally to the squares of n_1, u_1 and Φ_1. Change independent variables from (t, z) to (τ, η) where

$$\begin{aligned} \eta &= \sqrt{2}\varepsilon^{1/2}\lambda_D^{-1}[z - (k_B T_e/m_p)^{1/2} t] \ , \\ \tau &= \sqrt{2}\varepsilon^{3/2}\omega_{pp} t \ . \end{aligned} \tag{20.41}$$

By substituting Eqs. (20.40) and (20.41) into the nonlinear equations (20.38) and equating terms of the same order in ε, show that n_1, u_1, Φ_1 *each* satisfy the Korteweg-de Vries equation (16.32):

$$\frac{\partial \zeta}{\partial \tau} + \zeta \frac{\partial \zeta}{\partial \eta} + \frac{\partial^3 \zeta}{\partial \eta^3} = 0 \ . \tag{20.42}$$

(b) In Sec. 16.3 we discussed the exact, single-soliton solution (16.33) to this KdV equation. Show that for an ion-acoustic soliton, this solution propagates with the physical speed $(1 + n_{1o})(k_B T_e/m_p)^{1/2}$ (where n_{1o} is the value of n_1 at the peak of the soliton), which is greater the larger is the wave's amplitude n_{1o}.

****

20.5 Wave Modes in a Cold, Magnetized Plasma

20.5.1 Dielectric Tensor and Dispersion Relation

TO HERE

We now complicate matters somewhat by introducing a uniform magnetic field $\mathbf{B}_0$ into the unperturbed plasma. To avoid further complications, we make the plasma cold, i.e. we omit thermal effects. The linearized equation of motion (20.13b) for each species then becomes

$$-i\omega \mathbf{u}_s = \frac{q_s \mathbf{E}}{m_s} + \frac{q_s}{m_s} \mathbf{u}_s \times \mathbf{B}_0 \ . \tag{20.43}$$

It is convenient to multiply this equation of motion by $n_s q_s/\epsilon_0$ and introduce a scalar plasma frequency and scalar and vectorial cyclotron frequencies for each species

$$\boxed{\omega_{ps} = \left(\frac{n_s q_s^2}{\epsilon_0 m_s}\right)^{1/2} \ , \quad \omega_{cs} = \frac{q_s B_0}{m_s} \ , \quad \boldsymbol{\omega}_{cs} = \omega_{cs}\hat{\mathbf{B}}_0 = \frac{q_s \mathbf{B}_0}{m_s}} \tag{20.44}$$

[2]See Box 7.2 for a discussion of such bookkeeping parameters in a different context.

[so $\omega_{pp} = \sqrt{(m_e/m_p)}\,\omega_{pe} \simeq \omega_{pe}/43$, $\omega_{ce} < 0$, $\omega_{cp} > 0$, and $\omega_{cp} = (m_e/m_p)|\omega_{ce}| \simeq |\omega_{ce}|/1860$]. Thereby we bring the equation of motion (20.43) into the form

$$-i\omega\left(\frac{nq_s}{\epsilon_0}\mathbf{u}_s\right) + \boldsymbol{\omega}_{cs}\times\left(\frac{nq_s}{\epsilon_0}\mathbf{u}_s\right) = \omega_{ps}^2\mathbf{E}\,. \tag{20.45}$$

By combining this equation with $\boldsymbol{\omega}_{cs}\times$(this equation), we can solve for the fluid velocity of species s as a linear function of the electric field $\mathbf{E}$:

$$\boxed{\frac{n_s q_s}{\epsilon_0}\mathbf{u}_s = -i\left(\frac{\omega\omega_{ps}^2}{\omega_{cs}^2-\omega^2}\right)\mathbf{E} - \frac{\omega_{ps}^2}{(\omega_{cs}^2-\omega^2)}\boldsymbol{\omega}_{cs}\times\mathbf{E} + \boldsymbol{\omega}_{cs}\frac{i\omega_{ps}^2}{(\omega_{cs}^2-\omega^2)\omega}\boldsymbol{\omega}_{cs}\cdot\mathbf{E}}\,. \tag{20.46}$$

(This relation is useful when one tries to deduce the physical properties of a wave mode.) From this fluid velocity we can read off the current $\mathbf{j} = \sum_s n_s q_s \mathbf{u}_s$ as a linear function of $\mathbf{E}$; by comparing with Ohm's law $\mathbf{j} = \boldsymbol{\kappa}_{\rm e}\cdot\mathbf{E}$, we then obtain the tensorial conductivity $\boldsymbol{\kappa}_{\rm e}$, which we insert into Eq. (20.21) to get the following expression for the dielectric tensor (in which $\mathbf{B}_0$ and thence $\boldsymbol{\omega}_{cs}$ is taken to be along the z axis):

$$\boldsymbol{\epsilon} = \begin{pmatrix} \epsilon_1 & -i\epsilon_2 & 0 \\ i\epsilon_2 & \epsilon_1 & 0 \\ 0 & 0 & \epsilon_3 \end{pmatrix}\,, \tag{20.47}$$

where

$$\boxed{\epsilon_1 = 1 - \sum_s \frac{\omega_{ps}^2}{\omega^2-\omega_{cs}^2}\,,\quad \epsilon_2 = \sum_s \frac{\omega_{ps}^2\omega_{cs}}{\omega(\omega^2-\omega_{cs}^2)}\,,\quad \epsilon_3 = 1 - \sum_s \frac{\omega_{ps}^2}{\omega^2}}\,. \tag{20.48}$$

Let the wave propagate in the x–z plane, at an angle θ to the z-axis (i.e. to the magnetic field). Then the algebratized wave operator (20.8) takes the form

$$||L_{ij}|| = \frac{\omega^2}{c^2}\begin{pmatrix} \epsilon_1 - \mathfrak{n}^2\cos^2\theta & -i\epsilon_2 & \tilde{n}^2\sin\theta\cos\theta \\ i\epsilon_2 & \epsilon_1 - \mathfrak{n}^2 & 0 \\ \mathfrak{n}^2\sin\theta\cos\theta & 0 & \epsilon_3 - \tilde{n}^2\sin^2\theta \end{pmatrix}\,, \tag{20.49}$$

where

$$\boxed{\mathfrak{n} = \frac{ck}{\omega}} \tag{20.50}$$

is the wave's index of refraction—i.e, the wave's phase velocity is $V_{\rm ph} = \omega/k = c/\mathfrak{n}$. (Note: $\mathfrak{n}$ must not be confused with the number density of particles n.) The algebratized wave operator (20.49) will be needed when we explore the physical nature of modes, in particular the directions of their electric fields, which satisfy $L_{ij}E_j = 0$.

From the wave operator (20.49), we deduce the waves' dispersion relation $\det||L_{ij}|| = 0$. Some algebra brings this into the form

$$\boxed{\tan^2\theta = \frac{-\epsilon_3(\mathfrak{n}^2-\epsilon_R)(\mathfrak{n}^2-\epsilon_L)}{\epsilon_1(\mathfrak{n}^2-\epsilon_3)\,(\mathfrak{n}^2-\epsilon_R\,\epsilon_L/\epsilon_1)}}\,, \tag{20.51}$$

where

$$\boxed{\epsilon_L = \epsilon_1 - \epsilon_2 = 1 - \sum_s \frac{\omega_{ps}^2}{\omega(\omega - \omega_{cs})} \ , \quad \epsilon_R = \epsilon_1 + \epsilon_2 = 1 - \sum_s \frac{\omega_{ps}^2}{\omega(\omega + \omega_{cs})}} \ . \tag{20.52}$$

20.5.2 Parallel Propagation

As a first step in making sense out of the general dispersion relation (20.51) for waves in a cold, magnetized plasma, let us consider wave propagation along the magnetic field, so $\theta = 0$. The dispersion relation (20.51) then factorizes to give three pairs of solutions:

$$\mathfrak{n}^2 \equiv \frac{c^2k^2}{\omega^2} = \epsilon_L \ , \quad \mathfrak{n}^2 \equiv \frac{c^2k^2}{\omega^2} = \epsilon_R \ , \quad \epsilon_3 = 0 \ . \tag{20.53}$$

Consider the first solution in Eq. (20.53), $\mathfrak{n}^2 = \epsilon_L$. The algebratized wave equation $L_{ij}E_j = 0$ [with L_{ij} given by Eq. (20.49)] in this case requires that the electric field direction be $\mathbf{E} \propto (\mathbf{e}_x - i\mathbf{e}_y)e^{-i\omega t}$, which is a left-hand circularly polarized wave propagating along the static magnetic field (z direction). The second solution in (20.53), $\mathfrak{n}^2 = \epsilon_R$, is the corresponding right-hand circular polarized mode. From Eqs. (20.52) we see that these two modes propagate with different phase velocities (but only slightly different, if ω is far from the electron cyclotron frequency and far from the proton cyclotron frequency.) The third solution in (20.53), $\epsilon_3 = 0$, is just the electrostatic plasma oscillation in which the electrons and protons oscillate parallel to and are unaffected by the static magnetic field.

As an aid to exploring the frequency dependence of the left and right modes, we plot in Fig. 20.3 the refractive index $\mathfrak{n} = ck/\omega$ as a function of $\omega/|\omega_{ce}|$.

In the high-frequency limit, the refractive index for both modes is slightly less than unity and approaches that for an unmagnetized plasma, $\mathfrak{n} = ck/\omega \simeq 1 - \frac{1}{2}\omega_p^2/\omega^2$ [cf. Eq. (20.28)], but with a small difference between the modes given to leading order by

$$\mathfrak{n}_L - \mathfrak{n}_R \simeq \frac{\omega_{pe}^2\omega_{ce}}{\omega^3} \tag{20.54}$$

This difference is responsible for an important effect known as *Faraday rotation*:

Suppose that a linearly polarized wave is incident upon a magnetized plasma and propagates parallel to the magnetic field. We can deduce the behavior of the polarization by expanding the mode as a linear superposition of the two circular polarized eigenmodes, left and right. These two modes propagate with slightly different phase velocities, so after propagating some distance through the plasma, they acquire a relative phase shift $\Delta\phi$. When one then reconstitutes the linear polarized mode from the circular eigenmodes, this phase shift is manifest in a rotation of the plane of polarization through an angle $\Delta\phi/2$ (for small $\Delta\phi$). This, together with the difference in refractive indices (20.54) (which determines $\Delta\phi$) implies a rotation rate for the plane of polarization given by

$$\frac{d\chi}{dz} = \frac{\omega_{pe}^2\omega_{ce}}{2\omega^2 c} \ . \tag{20.55}$$

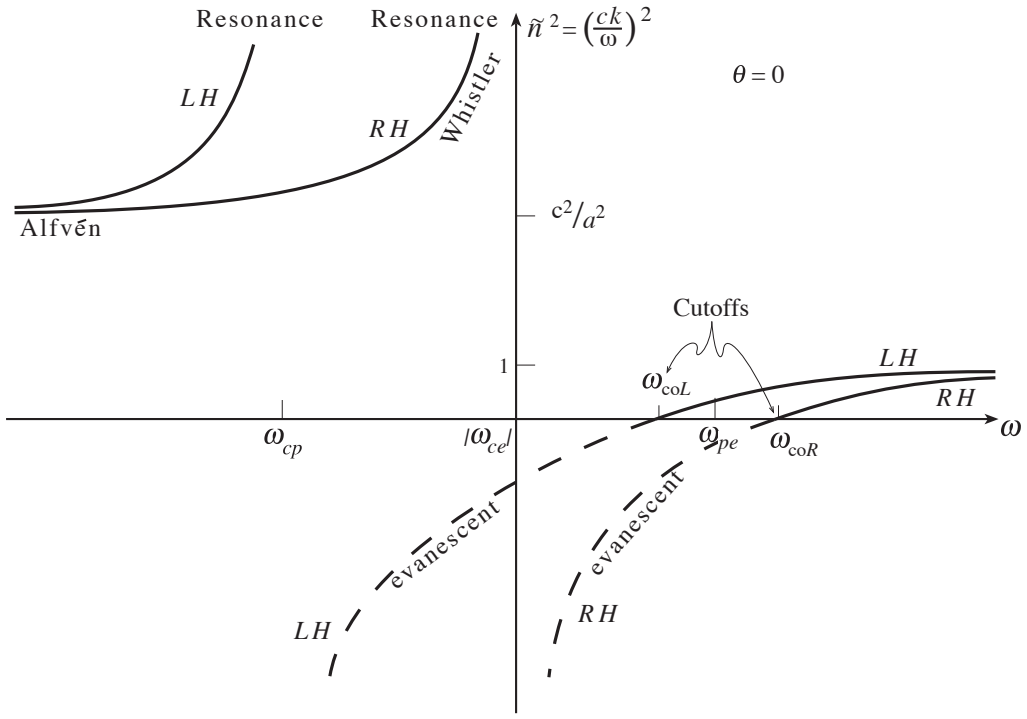

Fig. 20.3: Square of wave refractive index for circularly polarized waves propagating along the static magnetic field in a proton-electron plasma with $\omega_{pe} > \omega_{ce}$. (Remember, that we will regard both the electron and the proton cyclotron frequencies as positive numbers.) The angular frequency is plotted logarithmically in units of the modulus of the electron gyro frequency.

As the wave frequency is reduced, the refractive index decreases to zero, first for the right circular wave, then for the left circular wave; cf. Fig. 20.3. Vanishing of $\mathfrak{n}$ at a finite frequency corresponds to vanishing of k and infinite wavelength, i.e., it signals a *cutoff*; cf. Fig. 20.2 and associated discussion. When the frequency is lowered further, the squared refractive index becomes negative and the wave mode becomes evanescent. Correspondingly, when a circularly polarized electromagnetic wave with constant real frequency propagates into an inhomogeneous plasma parallel to its density gradient and parallel to a magnetic field, then beyond the spatial location of the wave's cutoff, its wave number k becomes purely imaginary, and the wave dies out with distance (gradually at first, then more rapidly).

The cutoff frequencies are different for the two modes and are given by

$$\omega_{\mathrm{co}R,L} = \frac{1}{2}\left[\left\{(\omega_{ce}+\omega_{cp})^2 + 4(\omega_{pe}^2+\omega_{pp}^2)\right\}^{1/2} \pm (|\omega_{ce}|-\omega_{cp})\right]$$
$$\simeq \omega_{pe} \pm |\omega_{ce}| \quad \text{if} \quad \omega_{pe} \gg |\omega_{ce}| \quad \text{as is usually the case.} \tag{20.56}$$

As we lower the frequency further (Fig. 20.3), first the right mode and then the left regain the ability to propagate. When the wave frequency lies between the proton and electron gyro frequencies, $\omega_{cp} < \omega < |\omega_{ce}|$, only the right mode propagates. This mode is sometimes called a *whistler*. As the mode's frequency increases toward the electron gyro frequency $|\omega_{ce}|$ (where it first recovered the ability to propagate), its refractive index and wave

vector become infinite—a signal that $\omega = |\omega_{ce}|$ is a *resonance* for the whistler; cf. Fig. 20.2. The physical origin of this resonance is that the wave frequency becomes resonant with the gyrational frequency of the electrons that are orbiting the magnetic field in the same sense as the wave's electric vector rotates. To quantify the strong wave absorption that occurs at this resonance, one must carry out a kinetic-theory analysis that takes account of the electrons' thermal motions (Chap. 21).

Another feature of the whistler is that it is highly dispersive close to resonance; its dispersion relation there is given approximately by

$$\omega \simeq \frac{|\omega_{ce}|}{1 + \omega_{pe}^2/c^2k^2} \tag{20.57}$$

The group velocity, obtained by differentiating Eq. (20.57), is given approximately by

$$\mathbf{V}_g = \nabla_{\mathbf{k}}\,\omega \simeq \frac{2\omega_{ce}c}{\omega_{pe}}\left(1 - \frac{\omega}{|\omega_{ce}|}\right)^{3/2}\hat{\mathbf{B}}_0\ . \tag{20.58}$$

This velocity varies extremely rapidly close to resonance, so waves of different frequency propagate at very different speeds.

This is the physical origin of the phenomenon by which whistlers were discovered, historically. They were first encountered by radio operators who heard, in their earphones, strange tones with rapidly changing pitch. These turned out to be whistler modes excited by lightning in the southern hemisphere, that propagated along the earth's magnetic field through the magnetosphere to the northern hemisphere. Only modes below the lowest electron gyro frequency on the waves' path (their geometric-optics ray) could propagate, and these were highly dispersed, with the lower frequencies arriving first.

There is also a resonance associated with the left hand polarized wave, which propagates below the proton cyclotron frequency; see Fig. 20.3.

Finally, let us examine the very low-frequency limit of these waves (Fig. 20.3). We find that both dispersion relations $\mathfrak{n}^2 = \epsilon_L$ and $\mathfrak{n}^2 = \epsilon_R$ asymptote, at arbitrarily low frequencies, to

$$\omega = ak\left(1 + \frac{a^2}{c^2}\right)^{-1/2}\ . \tag{20.59}$$

Here $a = B_0[\mu_0 n_e(m_p + m_e)]^{-1/2}$ is the Alfvén speed that arose in our discussion of magnetohydrodynamics [Eq. (18.64)]. In fact, both modes, left and right, at very low frequencies, have become the Alfvén waves that we studied using MHD in Sec. 18.7.2. However, our two-fluid formalism reports a phase speed $\omega/k = a/\sqrt{1 + a^2/c^2}$ for these Alfvén waves that is slightly lower than the speed $\omega/k = a$ predicted by our MHD formalism. The $1/\sqrt{1 + a^2/c^2}$ correction could not be deduced using nonrelativistic MHD, because that formalism neglects the displacement current. (Relativistic MHD includes the displacement current and predicts precisely this correction factor.)

We can understand the physical origin of this correction by examining the particles' motions in a very-low-frequency Alfvén wave; see Fig. 20.4. Because the wave frequency is far below both the electron and the proton cyclotron frequencies, both types of particle orbit the $\mathbf{B}_0$ field many times in a wave period. When the wave's slowly changing electric field is

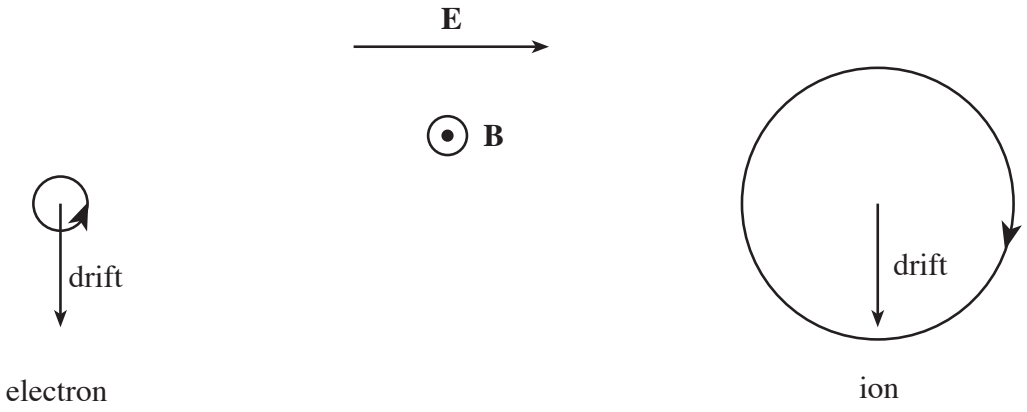

Fig. 20.4: Gyration of electrons and ions in a low frequency Alfvén wave. Although the electrons and ions gyrate with opposite senses about the magnetic field, their $\mathbf{E} \times \mathbf{B}$ drifts are similar. It is only in the next highest order of approximation that a net ion current is produced parallel to the applied electric field.

applied, the guiding centers of both types of orbits acquire the same slowly changing drift velocity $\mathbf{v} = \mathbf{E} \times \mathbf{B}_0/B_0^2$, so the two fluid velocities also drift at this rate and the currents associated with the proton and electron drifts cancel. However, when we consider corrections to the guiding-center response that are of higher order in ω/ω_{cp} and ω/ω_{ce}, we find that the ions drift slightly faster than the electrons, which produces a net current that modifies the magnetic field and gives rise to the $1/\sqrt{1 + a^2/c^2}$ correction to the Alfvén wave's phase speed.

20.5.3 Perpendicular Propagation

Turn, next, to waves that propagate perpendicular to the static magnetic field, ($\mathbf{k} = k\mathbf{e}_x$; $\mathbf{B}_0 = B_0\mathbf{e}_z$; $\theta = \pi/2$). In this case our general dispersion relation (20.51) again has three solutions corresponding to three modes:

$$\mathfrak{n}^2 \equiv \frac{c^2k^2}{\omega^2} = \epsilon_3 \ , \quad \mathfrak{n}^2 \equiv \frac{c^2k^2}{\omega^2} = \frac{\epsilon_R\epsilon_L}{\epsilon_1} \ , \quad \epsilon_1 = 0 \ . \tag{20.60}$$

The first solution

$$\mathfrak{n}^2 = \epsilon_3 = 1 - \frac{\omega_p^2}{\omega^2} \tag{20.61}$$

has the same index of refraction as for an electromagnetic wave in an unmagnetized plasma [cf. Eq. (20.25)], so this is called the *ordinary mode*. In this mode, the electric vector and velocity perturbation are parallel to the static magnetic field, so the field has no influence on the wave. The wave is identical to an electromagnetic wave in an unmagnetized plasma.

The second solution in Eq. (20.60),

$$\mathfrak{n}^2 = \epsilon_R\epsilon_L/\epsilon_1 = \frac{\epsilon_1^2 - \epsilon_2^2}{\epsilon_1} \ , \tag{20.62}$$

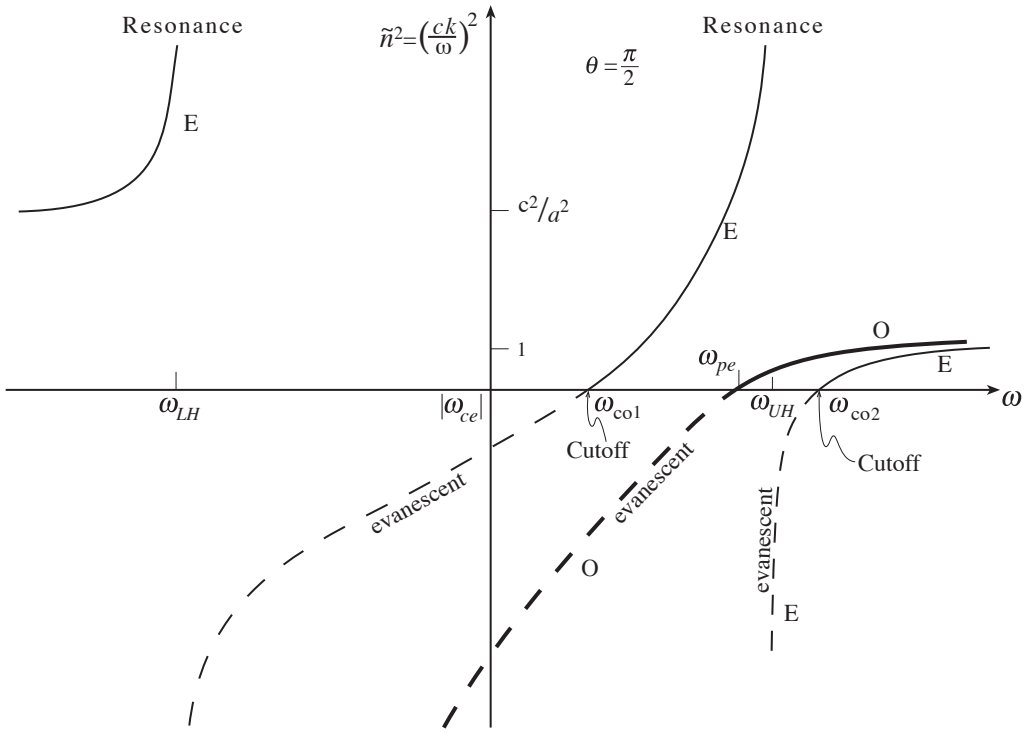

Fig. 20.5: Variation of refractive index $\mathfrak{n}$ for wave propagation perpendicular to the magnetic field in an electron ion plasma with $\omega_{pe} > \omega_{ce}$. The ordinary mode is designated by O, the extraordinary mode by E.

is known as the *extraordinary mode* and has an electric field that is orthogonal to $\mathbf{B}_0$ but not to $\mathbf{k}$.

The refractive indices for the ordinary and extraordinary modes are plotted as functions of frequency in Fig. 20.5. The ordinary-mode curve is dull; it is just like that in an unmagnetized plasma. The extraordinary-mode curve is more interesting. It has two cutoffs, with frequencies

$$\omega_{co1,2} \simeq \left(\omega_{pe}^2 + \frac{1}{4}\omega_{ce}^2\right)^{1/2} \pm \frac{1}{2}\omega_{ce} \ , \tag{20.63}$$

and two resonances with strong absorption, at frequencies known as the *Upper and Lower Hybrid* frequencies. These frequencies are given approximately by

$$\begin{aligned} \omega_{UH} &\simeq (\omega_{pe}^2 + \omega_{ce}^2)^{1/2} \ , \\ \omega_{LH} &\simeq \left[\frac{(\omega_{pe}^2 + |\omega_{ce}|\omega_{cp})|\omega_{ce}|\omega_{cp}}{\omega_{pe}^2 + \omega_{ce}^2}\right]^{1/2} \ . \end{aligned} \tag{20.64}$$

In the limit of very low frequency, the extraordinary, perpendicularly propagating mode has the same dispersion relation $\omega = ak/\sqrt{1 + a^2/c^2}$ as the paralleling propagating modes

[Eq. (20.59)]. It has become the fast magnetosonic wave, propagating perpendicular to the static magnetic field (Sec. 18.7.2), while the parallel waves became the Alfvén modes.

20.6 Propagation of Radio Waves in the Ionosphere

The discovery, in 1902, that radio waves could be reflected off the ionosphere, and thereby could be transmitted over long distances, revolutionized communications and stimulated intensive research on radio wave propagation in a magnetized plasma. In this section, we shall discuss radio-wave propagation in the ionosphere, for waves whose propagation vectors make arbitrary angles θ to the magnetic field. The approximate formalism we shall develop is sometimes called *magneto-ionic theory*.

The ionosphere is a dense layer of partially ionized gas between 50 and 300 km above the surface of the earth. The ionization is due to incident solar UV radiation. Although the ionization fraction increases with height, the actual density of free electrons passes through a maximum whose height rises and falls with the sun.

The electron gyro frequency varies from ~ 0.5 to ~ 1 MHz in the ionosphere, and the plasma frequency increases from effectively zero to a maximum that can be as high as 100 MHz; so typically, $\omega_{pe} \gg |\omega_{ce}|$. We are interested in wave propagation at frequencies above the electron plasma frequency, which in turn is well in excess of the ion plasma frequency and the ion gyro frequency. It is therefore a good approximation to ignore ion motions altogether. In addition, at the altitudes of greatest interest for radio wave propagation, the temperature is very low, $T_e \sim 200 - 600$K, so the cold plasma approximation is well justified. A complication that one must sometimes face in the ionosphere is the influence of collisions (Ex. 20.3 above), but in this section we shall ignore it.

It is conventional in magnetoionic theory to introduce two dimensionless parameters

$$X = \frac{\omega_{pe}^2}{\omega^2} , \quad Y = \frac{|\omega_{ce}|}{\omega} , \tag{20.65}$$

in terms of which (ignoring ion motions) the components (20.48) of the dielectric tensor (20.47) are

$$\epsilon_1 = 1 + \frac{X}{Y^2 - 1} , \quad \epsilon_2 = \frac{XY}{Y^2 - 1} , \quad \epsilon_3 = 1 - X . \tag{20.66}$$

It is convenient, in this case, to rewrite the dispersion relation $\det||L_{ij}|| = 0$ in a form different from Eq. (20.51)—a form derivable, e.g., by computing explicitly the determinant of the matrix (20.49), setting

$$x = \frac{X - 1 + \mathfrak{n}^2}{1 - \mathfrak{n}^2} , \tag{20.67}$$

solving the resulting quadratic in x, then solving for $\mathfrak{n}^2$. The result is the *Appleton-Hartree* dispersion relation

$$\mathfrak{n}^2 = 1 - \frac{X}{1 - \frac{Y^2 \sin^2\theta}{2(1-X)} \pm \left[\frac{Y^4 \sin^4\theta}{2(1-X)^2} + Y^2 \cos^2\theta\right]^{1/2}} \tag{20.68}$$

There are two commonly used approximations to this dispersion relation. The first is the *quasi-longitudinal* approximation, which is used when $\mathbf{k}$ is approximately parallel to the static magnetic field, i.e. when θ is small. In this case, just retaining the dominant terms in the dispersion relation, we obtain

$$\mathfrak{n}^2 \simeq 1 - \frac{X}{1 \pm Y\cos\theta} \ . \tag{20.69}$$

This is just the dispersion relation (20.53) for the left and right modes in strictly parallel propagation, with the substitution $B_0 \to B_0\cos\theta$. By comparing the magnitude of the terms that we dropped from the full dispersion relation in deriving (20.69) with those that we retained, one can show that the quasi-longitudinal approximation is valid when

$$Y^2\sin^2\theta \ll 2(1-X)\cos\theta \ . \tag{20.70}$$

The second approximation is the *quasi-transverse* approximation; it is appropriate when inequality (20.70) is reversed. In this case the two modes are generalizations of the precisely perpendicular ordinary and extraordinary modes, and their approximate dispersion relations are

$$\begin{aligned} \mathfrak{n}_O^2 &= 1 - X \ , \\ \mathfrak{n}_X^2 &= 1 - \frac{X(1-X)}{1 - X - Y^2\sin^2\theta} \ . \end{aligned} \tag{20.71}$$

The ordinary-mode dispersion relation is unchanged from the strictly perpendicular one, (20.61); the extraordinary dispersion relation is obtained from the strictly perpendicular one (20.62) by the substitution $B_0 \to B_0\sin\theta$.

The quasi-longitudinal and quasi-transverse approximations simplify the problem of tracing rays through the ionosphere.

Commercial radio stations operate in the AM (amplitude modulated) band (0.5-1.6 MHz), the SW (short wave) band (2.3-18 MHz), and the FM (frequency modulated) band (88-108 MHz). Waves in the first two bands are reflected by the ionosphere and can therefore be transmitted over large surface areas. FM waves, with their higher frequencies, are not reflected and must therefore be received as "ground waves" (waves that propagate directly, near the ground). However, they have the advantage of a larger bandwidth and consequently a higher fidelity audio output. As the altitude of the reflecting layer rises at night, short wave communication over long distances becomes easier.

****

EXERCISES

Exercise 20.6 *Derivation: Appleton-Hartree Dispersion Relation*
Derive Eq. (20.68).

Exercise 20.7 *Example: Dispersion and Faraday rotation of Pulsar pulses*
A radio pulsar emits regular pulses at 1s intervals, which propagate to Earth through the ionized interstellar plasma with electron density $n_e \simeq 3 \times 10^4 \mathrm{m}^{-3}$. The pulses observed at $f = 100$ MHz are believed to be emitted at the same time as those observed at much higher frequency, but they arrive with a delay of 100ms.

(a) Explain briefly why pulses travel at the group velocity instead of the phase velocity and show that the expected time delay of the $f = 100$ MHz pulses relative to the high-frequency pulses is given by

$$\Delta t = \frac{e^2}{8\pi^2 m_e \epsilon_0 f^2 c} \int n_e dx \ , \tag{20.72}$$

where the integral is along the waves' propagation path. Hence compute the distance to the pulsar.

(b) Now suppose that the pulses are linearly polarized and that their propagation is accurately described by the quasi-longitudinal approximation. Show that the plane of polarization will be Faraday rotated through an angle

$$\Delta\chi = \frac{e\Delta t}{m_e}\langle B_\parallel \rangle \tag{20.73}$$

where $\langle B_\parallel \rangle = \int n_e \mathbf{B}\cdot d\mathbf{x} / \int n_e dx$. The plane of polarization of the pulses emitted at 100 MHz is believed to be the same as the emission plane for higher frequencies, but when the pulses arrive at earth, the 100 MHz polarization plane is observed to be rotated through 3 radians relative to that at high frequencies. Calculate the mean parallel component of the interstellar magnetic field.

Exercise 20.8 *Example: Reflection of Short Waves by the Ionosphere*
The free electron density in the night-time ionosphere increases exponentially from $10^9 \mathrm{m}^{-3}$ to $10^{11} \mathrm{m}^{-3}$ as the altitude increases from 100 to 200km and diminishes above this height. Use Snell's law [Eq. (7.49)] to calculate the maximum range of 10 MHz waves transmitted from the earth's surface, assuming a single ionospheric reflection.

****

20.7 CMA Diagram for Wave Modes in a Cold, Magnetized Plasma

Magnetized plasmas are anisotropic, just like most nonlinear crystals (Chap. 10). This implies that the phase speed of a propagating wave mode depends on the angle between the direction of propagation and the magnetic field. There are two convenient ways to exhibit this anisotropy diagrammatically. The first method, due originally to Fresnel, is to construct

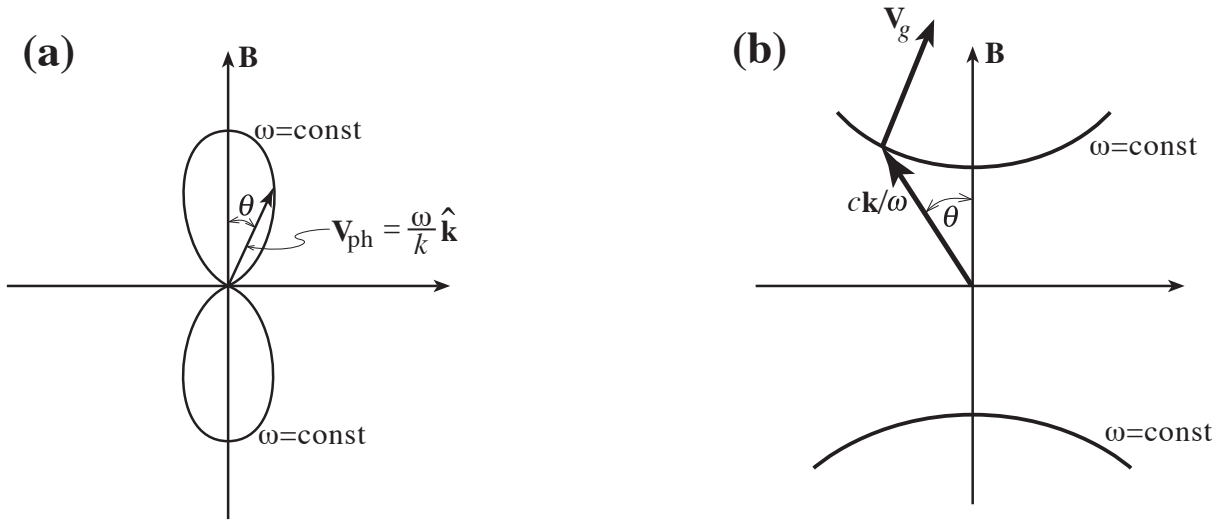

Fig. 20.6: (a) *Wave normal surface* for a whistler mode propagating at an angle θ with respect to the magnetic field direction. In this diagram we plot the phase velocity $\mathbf{V}_{\rm ph} = (\omega/k)\hat{\mathbf{k}}$ as a vector from the origin, with the direction of the magnetic field chosen upward. When we fix the frequency ω of the wave, the tip of the phase velocity vector sweeps out the figure-8 curve as its angle θ to the magnetic field changes. This curve should be thought of as rotated around the vertical (magnetic-field) direction to form a figure-8 "wave-normal" surface. Note that there are some directions where no mode can propagate. (b) *Refractive index surface* for the same whistler mode. Here we plot $c\mathbf{k}/\omega$ as a vector from the origin, and as its direction changes with fixed ω, this vector sweeps out the two hyperboloid-like surfaces. Since the length of the vector is $ck/\omega = \mathfrak{n}$, this figure can be thought of as a polar plot of the refractive index $\mathfrak{n}$ as a function of wave propagation direction θ for fixed ω; hence the name "refractive index surface". The group velocity $\mathbf{V}_g$ is orthogonal to the refractive-index surface (Ex. 20.10). Note that for this whistler mode, the energy flow (along $\mathbf{V}_g$) is focused toward the direction of the magnetic field.

phase velocity surfaces (also called *wave-normal surfaces*), which are polar plots of the wave phase velocity $V_{\rm ph} = \omega/k$ as a function of the angle θ that the wave vector $\mathbf{k}$ makes with the magnetic field; see Fig. 20.6a.

The second type of surface, used originally by Hamilton, is the *refractive index surface*. This is a polar plot of the refractive index $\mathfrak{n} = ck/\omega$ for a given frequency again as a function of the wave vector's angle θ to $\mathbf{B}$; see Fig. 20.6b. This plot has the important property that the group velocity is perpendicular to the surface (Ex. 20.10). As discussed above, the energy flow is along the direction of the group velocity and, in a magnetized plasma, this can make a large angle with the wave vector.

A particularly useful application of these ideas is to a graphical representation of the various types of wave modes that can propagate in a cold, magnetized plasma, Fig. 20.7. This is known as the *Clemmow-Mullaly-Allis* or *CMA* diagram. The character of waves of a given frequency ω depends on the ratio of this frequency to the plasma frequency and the cyclotron frequency. This allows us to define two dimensionless numbers, $(\omega_{pe}^2 + \omega_{pp}^2)/\omega^2$ and $|\omega_{ce}|\omega_{cp}/\omega^2$, which are plotted on the horizontal and vertical axes of the CMA diagram. [Recall that $\omega_{pp} = \omega_{pe}\sqrt{m_e/m_p}$ and $\omega_{cp} = \omega_{ce}(m_e/m_p)$.] The CMA space defined by these

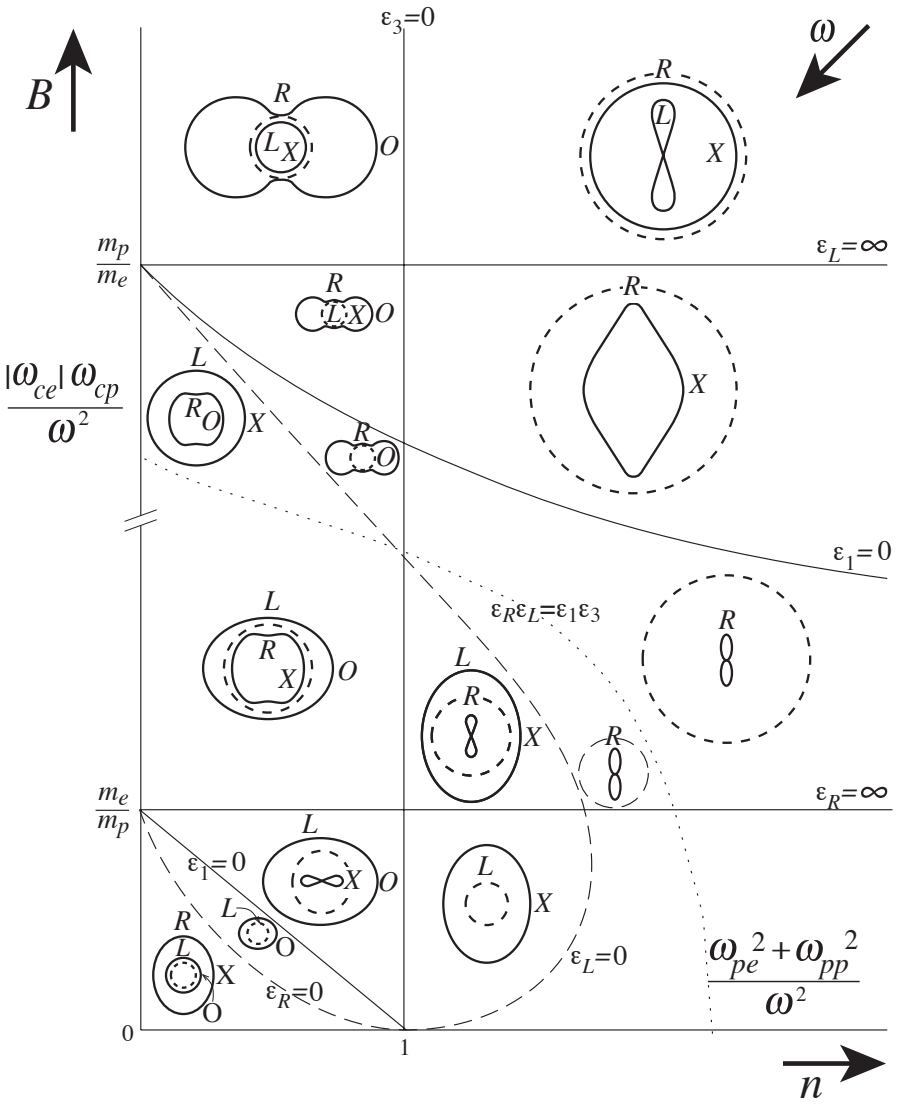

Fig. 20.7: Clemmow-Mullally-Allis (CMA) Diagram for wave modes with frequency ω propagating in a plasma with plasma frequencies ω_{pe}, ω_{pp} and gyro frequencies ω_{ce}, ω_{cp}. Plotted upward is the dimensionless quantity $|\omega_{ce}|\omega_{cp}/\omega^2$, which is proportional to B^2, so magnetic field strength also increases upward. Plotted rightward is the dimensionless quantity $(\omega_{pe}^2 + \omega_{pp}^2)/\omega^2$, which is proportional to n, so the plasma number density also increases rightward. Since both the ordinate and the abscissa scale as $1/\omega^2$, ω increases in the left-down direction. This plane is split into sixteen regions by a set of curves on which various dielectric components have special values. In each of the sixteen regions are shown two or one or no wave-normal surfaces (phase-velocity surfaces) at fixed ω; cf. Fig. 20.6a. These surfaces depict the types of wave modes that can propagate for that region's values of frequency ω, magnetic field strength B, and electron number density n. In each wave-normal diagram the dashed circle indicates the speed of light; a point outside that circle has phase velocity $V_{\rm ph}$ greater than c; inside the circle, $V_{\rm ph} < c$. The topologies of the wave normal surfaces and speeds relative to c are constant throughout each of the sixteen regions, and change as one moves between regions.

two dimensionless parameters can be subdivided into sixteen regions, within each of which the propagating modes have a distinctive character. The mode properties are indicated by sketching the topological form of the wave normal surfaces associated with each region.

The form of each wave-normal surface in each region can be deduced from the general dispersion relation (20.51). To deduce it, one must solve the dispersion relation for $1/\mathfrak{n} = \omega/kc = V_{\rm ph}/c$ as a function of θ and ω, and then generate the polar plot of $V_{\rm ph}(\theta)$.

On the CMA diagram's wave-normal curves, the characters of the parallel and perpendicular modes are indicated by labels: R and L for right and left parallel modes ($\theta = 0$), and O and X for ordinary and extraordinary perpendicular modes ($\theta = \pi/2$). As one moves across a boundary from one region to another, there is often a change of which parallel mode gets deformed continuously, with increasing θ, into which perpendicular mode. In some regions a wave-normal surface has a figure-eight shape, indicating that the waves can propagate only over a limited range of angles, $\theta < \theta_{\rm max}$. In some regions there are two wave-normal surfaces, indicating that—at least in some directions θ—two modes can propagate; in other regions there is just one wave-normal surface, so only one mode can propagate; and in the bottom-right two regions there are no wave-normal surfaces, since no waves can propagate at these high densities and low magnetic-field strengths.

****

EXERCISES

Exercise 20.9 *Problem: Exploration of Modes in the CMA Diagram*
For each of the following modes studied earlier in this chapter, identify in the CMA diagram the phase speed, as a function of frequency ω, and verify that the turning on and cutting off of the modes, and the relative speeds of the modes, are in accord with the CMA diagram's wave-normal curves.

a. EM modes in an unmagnetized plasma.

b. Left and right modes for parallel propagation in a magnetized plasma.

c. Ordinary and extraordinary modes for perpendicular propagation in a magnetized plasma.

Exercise 20.10 *Derivation: Refractive Index Surface*
Verify that the group velocity of a wave mode is perpendicular to the refractive index surface.

****

20.8 Two Stream Instability

When considered on large enough scales, plasmas behave like fluids and are subject to a wide variety of fluid dynamical instabilities. However, as we are discovering, plasmas have internal degrees of freedom associated with their velocity distributions, and this offers additional opportunities for unstable wave modes to grow and for free energy to be released. A full description of velocity-space instabilities is necessarily kinetic and must await the following chapter. However, it is instructive to consider a particularly simple example, the *two stream instability*, using cold plasma theory, as this brings out several features of the more general theory in a particularly simple manner.

We will apply our results in a slightly unusual way, to the propagation of fast electron beams through the slowly outflowing solar wind. These electron beams are created by coronal disturbances generated on the surface of the sun (specifically those associated with "Type III" radio bursts). The observation of these fast electron beams was initially a puzzle because plasma physicists knew that they should be unstable to the exponential growth of electrostatic waves. What we will do in this section is demonstrate the problem. What we will not do is explain what is thought to be its resolution, since that involves nonlinear plasma physics considerations beyond the scope of this book.[3]

Consider a simple, cold (i.e. with negligible thermal motions) electron-proton plasma at rest. Ignore the protons for the moment. We can write the dispersion relation for electron plasma oscillations in the form

$$\frac{\omega_{pe}^2}{\omega^2} = 1. \tag{20.74}$$

Now allow the ions also to oscillate about their mean positions. The dispersion relation is slightly modified to

$$\frac{\omega_p^2}{\omega^2} = \frac{\omega_{pe}^2}{\omega^2} + \frac{\omega_{pp}^2}{\omega^2} = 1 \tag{20.75}$$

[cf. Eq. (20.24)]. If we were to add other components (for example Helium ions), that would simply add extra terms to Eq. (20.75).

Next, return to Eq. (20.74) and look at it in a reference frame through which the electrons are moving with speed u. The observed wave frequency is then Doppler shifted and so the dispersion relation becomes

$$\frac{\omega_{pe}^2}{(\omega - ku)^2} = 1\ , \tag{20.76}$$

where ω is now the angular frequency measured in this new frame. It should be evident from this how to generalize Eq. (20.75) to the case of several cold streams moving with different speeds u_i. We simply add the terms associated with each component using angular frequencies that have been appropriately Doppler shifted:

$$\boxed{\frac{\omega_{p1}^2}{(\omega - ku_1)^2} + \frac{\omega_{p2}^2}{(\omega - ku_2)^2} + \cdots = 1\ .} \tag{20.77}$$

(This procedure will be justified via kinetic theory in the next chapter.)

[3] See, e.g., Melrose 1980.

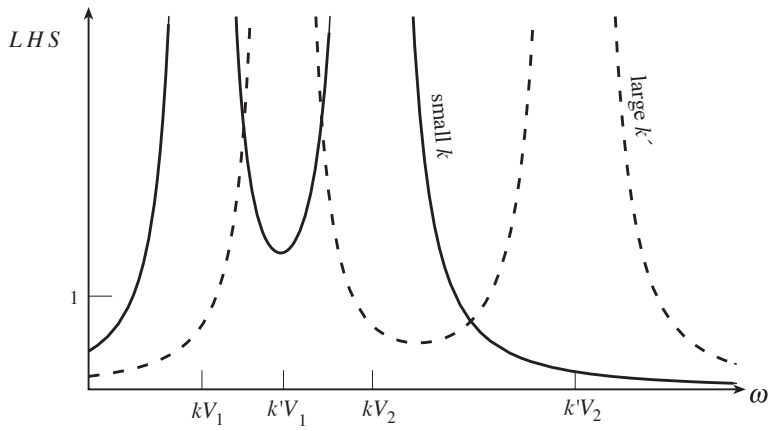

Fig. 20.8: Left hand side of the dispersion relation (20.77) for two cold plasma streams and two different choices of wave vector k. For small enough k, there are only two real roots for ω.

The left hand side of the dispersion relation (20.77) is plotted in Fig. 20.8 for the case of two cold plasma streams. The dispersion relation (20.77) is a quartic in ω and so it should have four roots. However, for small enough k only two of these roots will be real; cf. Fig. 20.8. The remaining two roots must be a complex conjugate pair and the root with the positive imaginary part corresponds to a growing mode. We have therefore shown that for small enough k the two stream plasma will be unstable. Small electrostatic disturbances will grow exponentially to large amplitude and ultimately react back upon the plasma. As we add more cold streams to the plasma, so we add more modes, some of which will be unstable. This simple example demonstrates how easy it is for a plasma to tap the free energy residing in anisotropic particle distribution functions.

Let us return to our solar-wind application and work in the rest frame of the wind ($u_1 = 0$) where the plasma frequency is $\omega_{p1} = \omega_p$. If the beam density is a fraction α of the solar wind density so $\omega_{p2}^2 = \alpha\omega_p^2$, and the beam velocity is $u_2 = V$, then by differentiating Eq. (20.77), we find that the local minimum of the left hand side occurs at $\omega = kV/(1+\alpha^{1/3})$, and the value of the left hand side at that minimum is $\omega_p^2(1+\alpha^{1/3})/\omega^2$. This minimum exceeds unity (thereby making two roots of the dispersion relation complex) for

$$k < \frac{\omega_p}{V}(1+\alpha^{1/3})^{3/2} \ . \tag{20.78}$$

This is therefore the condition for there to be a growing mode. The maximum value for the growth rate can be found simply by varying k. It is

$$\omega_i = \frac{3^{1/2}\alpha^{1/3}\omega_p}{2^{4/3}} \ . \tag{20.79}$$

For the solar wind near earth, we have $\omega_p \sim 10^5$rad s^{-1}, $\alpha \sim 10^{-3}$, $V \sim 10^4$km s^{-1}. We therefore find that the instability should grow, thereby damping the fast electron beam, in a length of 30km, which is much less than the distance from the sun (1.5×10^8 km)! This describes the problem that we will not resolve.

****

EXERCISES

Exercise 20.11 *Derivation: Two stream instability*
Verify Eq. (20.79)

Exercise 20.12 *Example: Relativistic Two Stream Instability*
In a very strong magnetic field, we can consider electrons as constrained to move in one dimension along the direction of the magnetic field. Consider a beam of relativistic protons propagating with density n_b and speed $u_b \sim c$ through a cold electron-proton plasma along $\mathbf{B}$. Generalize the dispersion relation (20.77) for modes with $\mathbf{k} \parallel \mathbf{B}$.

Exercise 20.13 *Problem: Drift Waves*
Another type of wave mode that can be found from a fluid description of a plasma (but which requires a kinetic treatment to understand completely) is a *drift wave*. The limiting case that we consider here is a modification of an ion acoustic mode in a strongly magnetized plasma with a density gradient. Suppose that the magnetic field is uniform and parallel to the direction $\mathbf{e}_z$. Let there be a gradient in the equilibrium density of both the electrons and the protons $n_0 = n_0(x)$. In the spirit of our description of ion acoustic modes in an unmagnetized, homogeneous plasma [cf. Eq. (20.36)], treat the ion fluid as cold but allow the electrons to be warm and isothermal with temperature T_e. We seek modes of frequency ω propagating perpendicular to the density gradient, i.e. with $\mathbf{k} = (0, k_y, k_z)$.

(i) Consider the equilibrium of the warm electron fluid and show that there must be a fluid drift velocity along the direction $\mathbf{e}_y$ of magnitude

$$V_{de} = -\frac{V_{ia}^2}{\omega_{ci}} \frac{1}{n_0} \frac{dn_0}{dx} \ , \tag{20.80}$$

where $V_{ia} = (k_B T_e/m_p)^{1/2}$ is the ion acoustic speed. Explain in physical terms the origin of this drift and why we can ignore the equilibrium drift motion for the ions.

(ii) We will limit our attention to low frequency electrostatic modes that have phase velocities below the Alfvén speed. Under these circumstances, perturbations to the magnetic field can be ignored and the electric field can be written as $\mathbf{E} = -\boldsymbol{\nabla}\Phi$. Write down the three components of the linearized ion equation of motion in terms of the perturbation to the ion density n, the ion fluid velocity $\mathbf{u}$ and the electrostatic potential Φ.

(iii) Write down the linearized equation of ion continuity, including the gradient in n_0, and combine with the equation of motion to obtain an equation for the fractional ion density perturbation

$$\frac{\delta n}{n_0} = \left(\frac{(\omega_{cp}^2 k_z^2 - \omega^2 k^2) V_{ia}^2 + \omega_{cp}^2 \omega k_y V_{de}}{\omega^2 (\omega_{cp}^2 - \omega^2)} \right) \cdot \left(\frac{e\Phi}{k_B T_e} \right) \tag{20.81}$$

(iv) Argue that the fractional electron density perturbation follows a linearized Boltzmann distribution so that

$$\frac{\delta n_e}{n_0} = \frac{e\Phi}{k_B T_e} \ . \tag{20.82}$$

(v) Use both the ion and the electron density perturbations in Poisson's equation to obtain the electrostatic drift wave dispersion relation in the low frequency ($\omega \ll \omega_{cp}$), long wavelength ($k\lambda_D \ll 1$) limit:

$$\omega = \frac{k_y V_{de}}{2} \pm \frac{1}{2}[k_y^2 V_{de}^2 + 4k_z^2 V_{ia}^2]^{1/2} \ . \tag{20.83}$$

Describe the physical character of the mode in the additional limit $k_z \to 0$. A proper justification of this procedure requires a kinetic treatment, which also shows that, under some circumstances, drift waves can be unstable and grow exponentially. Just as the two stream instability provides a mechanism for plasmas to erase non-uniformity in velocity space, so drift waves can rapidly remove spatial irregularities.

****

Bibliographic Note

The definitive monograph on waves in plasmas is Stix (1992). For the most elementary textbook treatment see portions of Chen (1974). For more sophisticated and detailed textbook treatments see Boyd and Sanderson (1969), Clemmow and Doughtery (1969), Krall and Trivelpiece (1973), Landau and Lifshitz (1981), and Schmidt (1966). For treatments that focus on astrophysical plasmas, see Melrose (1980) and Parks (1991).

Bibliography

Boyd, T. J. M. & Sanderson, J. J. 1969. *Plasma Dynamics*, London: Nelson.

Chen, F. F. 1974. *Introduction to Plasma Physics*, New York: Plenum.

Clemmow, P. C. & Dougherty, J. P. 1969. *Electrodynamics of Particles and Plasmas*, Reading: Addison-Wesley.

Krall, N. A. & Trivelpiece, A. W. 1973. *Principles of Plasma Physics*, New York: McGraw-Hill.

Landau, L. D. & Lifshitz, E. M. 1981. *Plasma Kinetics*, Oxford: Pergamon.

Melrose, D. B. 1980. *Plasma Astrophysics*, New York: Gordon and Breach.

Parks, G. K. 1991. *Physics of Space Plasmas*, Redwood City: Addison-Wesley.

Schmidt, G. 1966. *Physics of High Temperature Plasmas*, New York: Academic.

Stix, T. H. 1992. *Waves in Plasmas*, New York: American Institute of Physics.

Box 20.2
Important Concepts in Chapter 20

- For a linear dielectric medium: polarization vector $\mathbf{P}$, electrical susceptibility tensor χ_{ij}, dielectric tensor ϵ_{ij}, electrical conductivity tensor $\kappa_{\mathbf{e}\,ij}$, wave operator in Fourier domain L_{ij}, and dispersion relation $\det||L_{ij}|| = 0$, Sec. 20.2
- Two-fluid formalism for a plasma: for each species – fluid velocity $\mathbf{u}_s = \langle \mathbf{v}_s \rangle$, pressure tensor $\mathbf{P}_s$, particle conservation, and equation of motion (Euler equation plus Lorentz force), Sec. 20.3
- Waves in cold, unmagnetized plasma, Secs. 20.4.1, 20.4.2
  - How to deduce the electric field and particle motions in a wave mode, Secs. 20.4.1, 20.4.3
  - Electromagnetic waves and their cutoff at the plasma frequency, Secs. 20.4.2, 20.4.4
  - Nonpropagating electrostatic oscillations, Sec. 20.4.1
- Waves in warm, unmagnetized plasma:
  - Electrostatic oscillations become Langmuir waves, Sec. 20.4.3
  - Ion acoustic waves, Sec. 20.4.3
- *Cutoff:* form of dispersion relation near a cutoff; Electromagnetic waves and Langmuir waves as examples; for inhomogeneous plasma: deflection of wave away from cutoff region in space, Secs. 20.4.4, 20.6
- *Resonance:* form of dispersion relation near a resonance; Ion acoustic waves as example; for inhomogeneous plasma: attraction of wave into resonance region and dissipation there, Secs. 20.4.4, 20.6
- Waves in cold, magnetized plasma, Sec. 20.5
  - Waves propagating parallel to the magnetic field: Alfven waves, whistlers, right-circularly-polarized EM waves, and left-circularly-polarized EM waves, Sec. 20.5.2
  - Waves propagating perpendicular to the magnetic field: Magnetosonic waves, upper hybrid waves, lower hybrid waves, ordinary EM waves, extraordinary EM waves, Sec. 20.5.3
  - Ways to depict dependence of phase velocity on direction: phase-velocity (or wave-normal) surface and CMA diagram based on it; refractive index surface, Sec. 20.7
- Two-stream instability, Sec. 20.8